

REGULATORY INFORMATION DISTRIBUTION SYSTEM (RIDS)

ACCESSION NBR: 8301310142 DOC. DATE: 83/01/24 NOTARIZED: NO DOCKET #  
 FACIL: 50-244 Robert Emmet Ginna Nuclear Plant, Unit 1, Rochester G 05000244  
 AUTH. NAME AUTHOR AFFILIATION  
 MAIER, J. E. Rochester Gas & Electric Corp.  
 RECIP. NAME RECIPIENT AFFILIATION  
 CRUTCHFIELD, D. Operating Reactors Branch 5

SUBJECT: Forwards review of acoustic monitoring of steam generators during plant startup, Westinghouse metal impact monitoring sys recorded impacts from steam generator B. Signal characteristics did not indicate impacts in tubing.

DISTRIBUTION CODE: A001S COPIES RECEIVED: LTR 1 ENCL 1 SIZE: 45  
 TITLE: OR Submittal: General Distribution

NOTES: NRR/DL/SEP 1cy.

05000244

	RECIPIENT		COPIES			RECIPIENT		COPIES	
	ID	CODE/NAME	LTTR	ENCL		ID	CODE/NAME	LTTR	ENCL
INTERNAL:	NRR	ORBS BC 01	7	7					
		ELD/HDS4	1	0		NRR/DL DIR	1	1	
		NRR/DL/ORAB	1	0		NRR/DSI/RAB	1	1	
		REG FILE 04	1	1		RGN1	1	1	
EXTERNAL:	ACRS	09	6	6		LPDR	03	1	1
	NRC PDR	02	1	1		NSIC	05	1	1
	NTIS		1	1					
NOTES:			1	1					

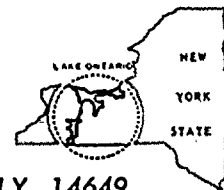
1. The first step in the process of identifying a problem is to determine the nature of the problem. This involves a thorough understanding of the situation and the factors that are contributing to the problem. Once the nature of the problem is understood, the next step is to identify the causes of the problem. This involves a detailed analysis of the situation and the factors that are contributing to the problem. Once the causes of the problem are identified, the next step is to develop a plan of action to address the problem. This involves determining the steps that need to be taken to solve the problem and the resources that will be required to implement the plan. Finally, the last step in the process is to implement the plan and monitor the results. This involves putting the plan into action and tracking the progress of the solution to ensure that the problem is resolved.

D. S. Jones

NOT RECORDED

[illegible]

201104



ROCHESTER GAS AND ELECTRIC CORPORATION • 89 EAST AVENUE, ROCHESTER, N.Y. 14649

JOHN E. MAIER  
Vice President

TELEPHONE  
AREA CODE 716 546-2700

January 24, 1983

Director of Nuclear Reactor Regulation  
Attention: Mr. Dennis M. Crutchfield; Chief  
Operating Reactors Branch No. 5  
U.S. Nuclear Regulatory Commission  
Washington, D.C. 20555

Subject: MIMS Performance During May 1982 Startup  
R. E. Ginna Nuclear Power Plant  
Docket No. 50-244

Dear Mr. Crutchfield:

As identified in Section 7.3 of our Steam Generator Evaluation Report dated April 26, 1982, a loose parts monitoring system was installed on both Ginna steam generators during the Spring 1982 outage. The system, a Westinghouse Metal Impact Monitoring System (MIMS), is described in our letter dated November 22, 1982.

During startup from our Spring 1982 outage, impacts were recorded on the MIMS from the B-Steam Generator. As described to you and your staff by telephone conversations during that startup and in a meeting with the NRC Staff on June 3, 1982, these signals were evaluated in detail and were determined to be originating at or very near the shell of the steam generator in the vicinity of the 5th support plate. Based on signal characteristic, it was determined to be very unlikely that the impacts were originating on steam generator tubing. We have now received that evaluation from Westinghouse which confirms and documents the findings that were presented to the NRC Staff on June 3. A final report is enclosed as attachment 1.

Further confirmation that the impacts were not affecting steam generator tubing was obtained during our interim outage, which began September 25, 1982. Multifrequency eddy current examination in the area of interest disclosed no tube wall degradation, thus demonstrating that there have been no impacts on these tubes. The examination included tubing on the cold leg of the B-Steam Generator from the tube sheet to the 6th support plate, from R1C1 to R44C38 and extending from all peripheral tubes inward by 2 to 3 rows.

A001-

8301310142 830124  
PDR ADOCK 05000244  
PDR



ROCHESTER GAS AND ELECTRIC CORP.

SHEET NO. 2

DATE January 24, 1983

TO Mr. Dennis M. Crutchfield

Based on the our evaluation and the eddy current inspection, we conclude that impacts recorded on the MIMS during the startup from our Spring outage 1982 are not the result of any mechanism which is affecting the integrity of the steam generator tubing.

Very truly yours;



John E. Maier

1944

1945

1946

1947

1948

1949

1950

1951

1952

1953

1954

1955

1956

REVIEW OF ACOUSTIC MONITORING OF  
STEAM GENERATORS DURING GINNA STARTUP,  
MAY 21 TO JUNE 2, 1982

SUMMARY OF RESULTS

As a result of RGE concern that no additional loose parts should remain in the Ginna Station steam generators, the latest model Westinghouse Digital Metal Impact Monitoring System was installed there in May, 1982. The design of this metal impact monitoring system has been demonstrated to yield much greater sensitivity to loose parts than required by regulatory guide 1.133, together with providing good false alarm and electrical noise rejection capabilities. The unit includes a tape recorder that automatically starts to record raw signal data on receipt of an alarm. The recorder uses a sufficiently high tape speed to allow complete impact signal waveform analysis and to maximize signal arrival time resolution for source triangulation. As originally installed, the system was configured with four sensors (accelerometers) mounted in a particular pattern near the tube sheets of each of the two generators. The design goal was to have high sensitivity to any impacts occurring on or near the tubesheet, and to have quick and easy primary-side versus secondary-side source discrimination.

As part of the process of system checkout and calibration measurements, various sizes of stainless-steel rods were used to impact each of the two steam generators. The data generated by these impacts provided reference sensitivity, frequency spectra, and arrival-time-difference information.





Monitoring by the MIM system began at plant heatup. During the heatup and pressurization some miscellaneous primary/secondary impact signals were detected, but work on various primary and secondary piping systems was still in progress - - for example, insulation was being reinstalled -- and the signals did not continue. However, at a very low power level (1 - 4%) a number of impact signals which could not be ascribed to any known operation were detected on steam generator B and recorded on magnetic tape. The signals were of significant amplitude, and recurred from time to time.

A detailed analysis of the impacts recorded on the first tape was therefore conducted that same evening. On that tape were four large amplitude ( $>10g$ ) impact signals occurring over a total period of about two minutes, but randomly spaced in time. All four signals had the same essential characteristics, namely the same relative waveform envelopes and the same relative arrival-time differences. From these data it was concluded that the source was not on the tubesheet or in the primary channel head region of the steam generator, but rather was fairly high in elevation. In particular, the received waveforms had clear first arrivals but long envelope rise times, indicative of a more distant source. The arrival-time differences between vertically-separated sensors was very large, while the arrival-time differences between horizontally-separated sensors was very small, also indicating the source to be some distance above the tube sheet.



As a result of that analysis, additional accelerometers were brought to the site and one was installed on a lifting lug at the top of the B steam generator. When impacts recurred following the installation of that sensor, the approximate elevation of the impact source was determined to be roughly 20 feet above the tube sheet. That it was the same general source area that had generated the previous activity was verified by review of waveforms and arrival times at the original four sensors.

To get better source location information, especially some circumferential resolution, two more sensors were mounted on lifting lugs at the feedwater line elevation just above the transition cone. The plant had increased power level by then and no further impacts were occurring, but one additional set of impacts was obtained by returning to a very low power level.

Triangulation calculations were then performed through analysis of arrival-time differences at the various sensors for each of the impact signals, after first creating an accurate map of the steam generator dimensions and sensor locations. The first arrivals of the acoustic waves turned out to be consistent at all of the sensors, so the source locations were determined to be nominally 21 to 24 feet in elevation above the top of the tubesheet and circumferentially within an arc bounded by the feedwater line angle and the closest tube lane (about a 60° arc). At this approximate elevation are, internally, the fifth support plate, and externally, a seismic support consisting of a ring girder attached to both the steam generator and to a series of snubbers.



From the analyses of the impact signals completed to date it can be concluded that the impact signals are probably thermal-mechanical in origin, on or near the steam generator shell, for the following reasons:

- 1) There are only a very few impacts, widely spaced in time, and having large amplitudes. A classical loose object would yield many more impacts and much wider amplitude variation.
- 2) The clean arrival times and excellent triangulations imply a source on or near the shell with no interfering or waveform-degrading acoustic paths.
- 3) The impact signals only occur at a very low power level.
- 4) The impacts occur in an area of the steam generator which is not normally considered a collection point for loose objects, and which contains a rather large and unique mechanical apparatus.

Additional data analysis has been performed to refine the on-site results. Triangulation calculations established error bounds by first replaying signal data through optimized filters, to obtain accurate timing information, and then by performing the triangulation on the computer, to accurately handle the steam generator geometry. Also, frequency spectra and other signal characteristics have been reviewed.



## ANALYSIS OF DATA

### 1. Introduction

At the time of the original analysis neither the effect of steam generator (SG) transition cone geometry on wave propagation nor the error bounds to be put on the triangulated locations could be analyzed exactly. In the error bounds case an extra problem was the need to determine more closely the impact signal arrival times and review carefully the acoustic wave propagation velocity experiment results.

A computer program has therefore been prepared which accurately calculates triangulation data and plots on a map of the steam generator the various curves corresponding to the distance differences between any two sensors. After some study it has also been possible, first, to determine upper and lower bounds on the effective wave propagation velocity, and second, to establish minimum and maximum arrival time differences between sensors for the actual impacts. The results are firm enough that bounding of the triangulation calculation can be stated to at least 90% confidence. The only ways that the confidence level could be increased further are through better positioning of sensors or by impact simulation directly in the zones calculated as sources.

Frequency spectrum analysis has also been performed on the impact signals to further characterize the source, based on the baseline data that had been obtained at temperature for several of the sensors. Since the source was concluded earlier to be on or near the shell, spectral analysis may indicate its characteristic length. In the case of a truly loose part the characteristic





length would then be proportional to mass, but no definite statement can be made from these impacts.

## 2. Data Analysis

### 2.1 Triangulation

Figures 1 and 2 are maps of the steam generator surface. The maps accurately show sensor locations and other features except within the transition cone, which is shown distorted. Particular features to be noted in Figure 1 include the elevation scale, which is referred to zero at the elevation of the lowest sensor (P), illustration of the tubesheet position; and indication of fourth support plate, fifth support plate, and snubber and ring girder positions.

One note on sensor locations: For good circumferential triangulation, there should be at least three sensors per elevation on a cylindrical structure to provide unique rather than dual solutions to triangulation calculations. The array shown is the closest approximation possible given the severe limitations on sensor placement after plant heatup.

Time traces of the four impacts that were analyzed following completed installation of the sensor array are shown in figures 3, 4, 5, and 6, which are copies of oscillograph traces. A total of six traces are included, although only four sensors were employed in the calculations. Sensors FL3, FL4, TH and S were used in the calculations while sensors P and T: were only used as supporting data. Typically the figures consist of a long period of background noise followed by the initial parts of the required



impact signals; a most important consideration was to characterize the noise so that the first signal arrivals could be discerned. The minimum and maximum distance differences are then presented in Table 1, which lists the best sensor pairs to use, the time-difference bounds, and the resulting distance-difference bounds, with maximum or minimum propagation velocities assumed as appropriate.

Once distance-difference bounds have been determined, the values can be used in the calculation and plotting of bounding curves on the steam generator map, illustrated in Figures 7 to 10 for the four cases. In each figure the SG map is shown with an elevation axis which coincides with the elevation axes of Figures 1 and 2. However, the rotational orientation is different from that of either Figure 1 or Figure 2; in Figures 7 to 10 the zero-degree line at the left edge is referred to the position of sensor FL3 and the tube lane. The feedwater line (off the top) is then at  $120^\circ$ , and sensor FL4 and the other side of the tube lane are at  $180^\circ$ . The grids on the plots are marked off in squares which are exactly two feet on a side, so the circumferential axis is not labeled in even degree values. Circumferential data is also taken to be at the half-thickness point of the wall for wave propagation use and is therefore slightly smaller than the surface dimension. Of major interest in each plot are the shaded regions, which represent the intersections of the bounding curve limits or possible source regions.



## 2.2 Frequency Spectrum Analysis

Part of the baseline data that were obtained during plant heatup was the simulation of loose part impacts at temperature. On this steam generator four different size steel rods were used to impact at a point approximately 110 inches from sensor TH and 215 inches from sensor S. Figures 11 to 14 illustrate the time signals and corresponding frequency characteristics of the detected impacts. The type of steel rods used is illustrated in Figure 15.

In a similar way the time signals and corresponding frequency spectra for the four impacts of RGE Tape 008 are shown in Figures 16 to 19. If these spectra are compared to the baseline data, the closest match of shape characteristics is with the 0.25 pound, 1 inch long rod. The implication is that, if the impacts are against the steam generator shell, a key characteristic length of the source is in the neighborhood of 1 inch. If the impacts are against an attached structure some combination of the source and structure provides a one inch characteristic.



TABLE 1  
ARRIVAL-TIME-DIFFERENCE ERROR BOUNDS  
RGE TAPE 008 METAL IMPACTS

<u>Footage</u>	<u>Sensor 1</u>	<u>Sensor 2</u>	<u><math>\Delta T</math> (divisions)</u>	<u><math>\Delta D</math> (feet)</u>
274	FL4	FL3	3.0 to 4.9	2.87 to 6.03
	TH	S	-0.9 to 1.9	-1.11 to 23.4
	FL4	S	7.5 to 8.7	7.17 to 10.71
400	TH	S	-1.3 to 1.0	-1.6 to 1.23
	FL3	TH	4.0 to 6.5	3.82 to 8.0
680	TH	S	1.1 to 2.9	1.05 to 3.57
	FL4	FL3	0.7 to 7.0	0.67 to 8.62
	FL3	TH	2.6 to 4.6	2.49 to 5.66
780	TH	S	1.5 to 2.8	1.43 to 3.45
	FL3	TH	0.3 to 1.9	0.29 to 2.34
	FL4	FL3	4.0 to 6.3	3.82 to 7.76

### 3.0 Conclusion

Computerized source location analysis has been completed for the set of RGE steam generator B impacts, but the triangulation plots show error bound areas which do not rule out either a single impact location or multiple impact locations. Because of both the signal-to-noise ratio and the difference in signal quality among the several impacts, the error bounds vary in size and region of coverage. If a single impact location is assumed, the intersection of all the error bound limits can be taken, but the initial result is a null set. However, upon expanding the bounds slightly, the region of maximum probability is centered at  $154^\circ$ , elevation 24 feet. If multiple impact points are assumed instead, the union of the error bound plots should be examined instead of the intersection. Taking only the three impacts that yielded a complete set of bounding curves -- that is, all impacts except the one at 400 feet on the tape -- there are five possible areas of consideration centered at the following coordinates: ( $140^\circ$ , 24 ft.), ( $160^\circ$ , 23 ft), ( $160^\circ$ , 25 ft), ( $190^\circ$ , 25 ft), and ( $230^\circ$ , 25 ft). If further analyses with greater accuracy are needed for any additional impacts, it is recommended that the following be performed: (1) Optimize the sensor locations and mountings for better circumferential resolution as noted earlier; (2) Conduct impact simulation in the area of interest.

In frequency spectrum analysis, the results indicate a characteristic dimension of one inch or less. "Characteristic dimension" is quoted rather than mass because it is not certain at this time whether or not the impacts are from an internal or external, loose or restrained source.





Figure 1. 47 13.3  
Map of Steam Generator

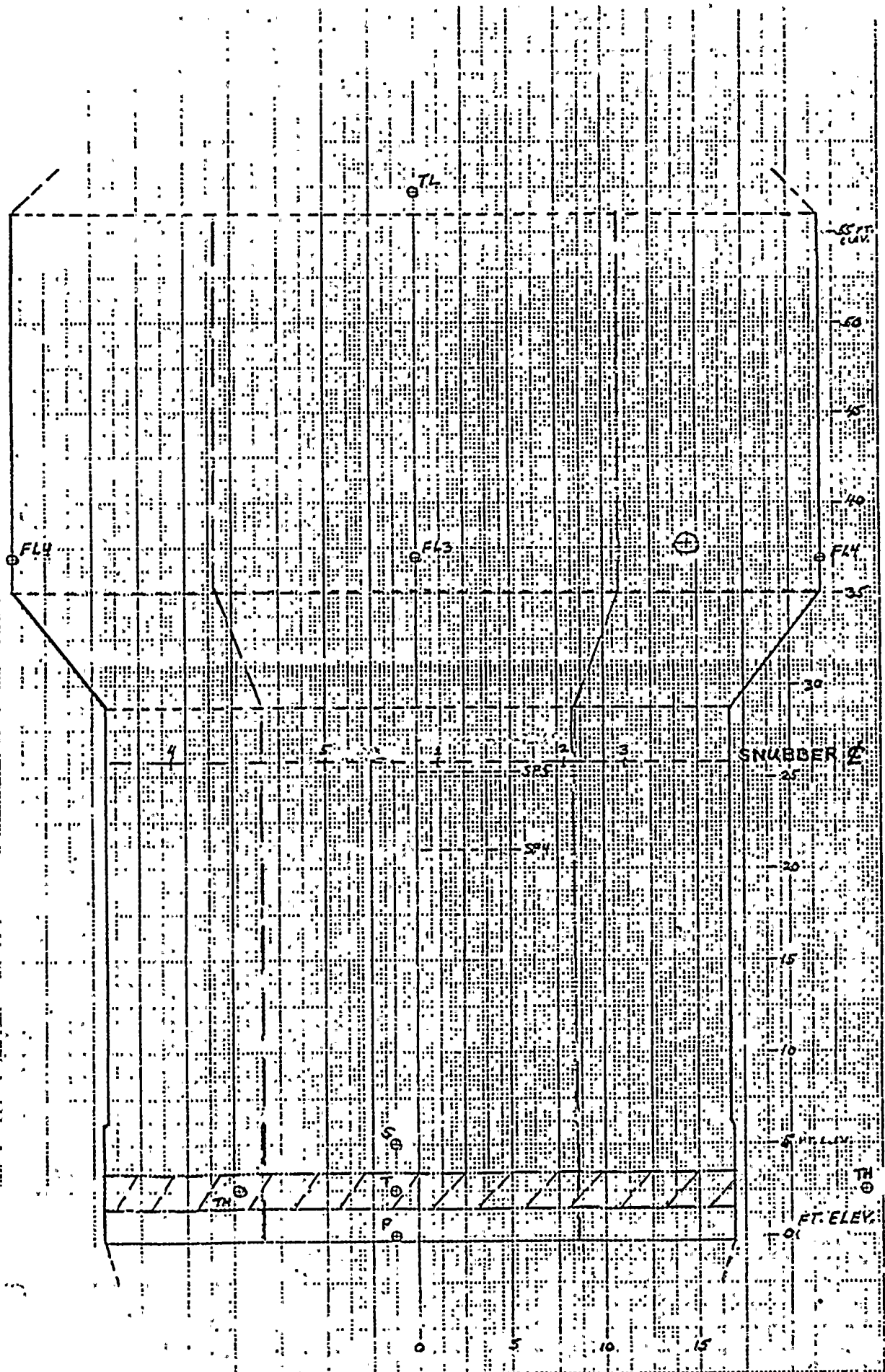
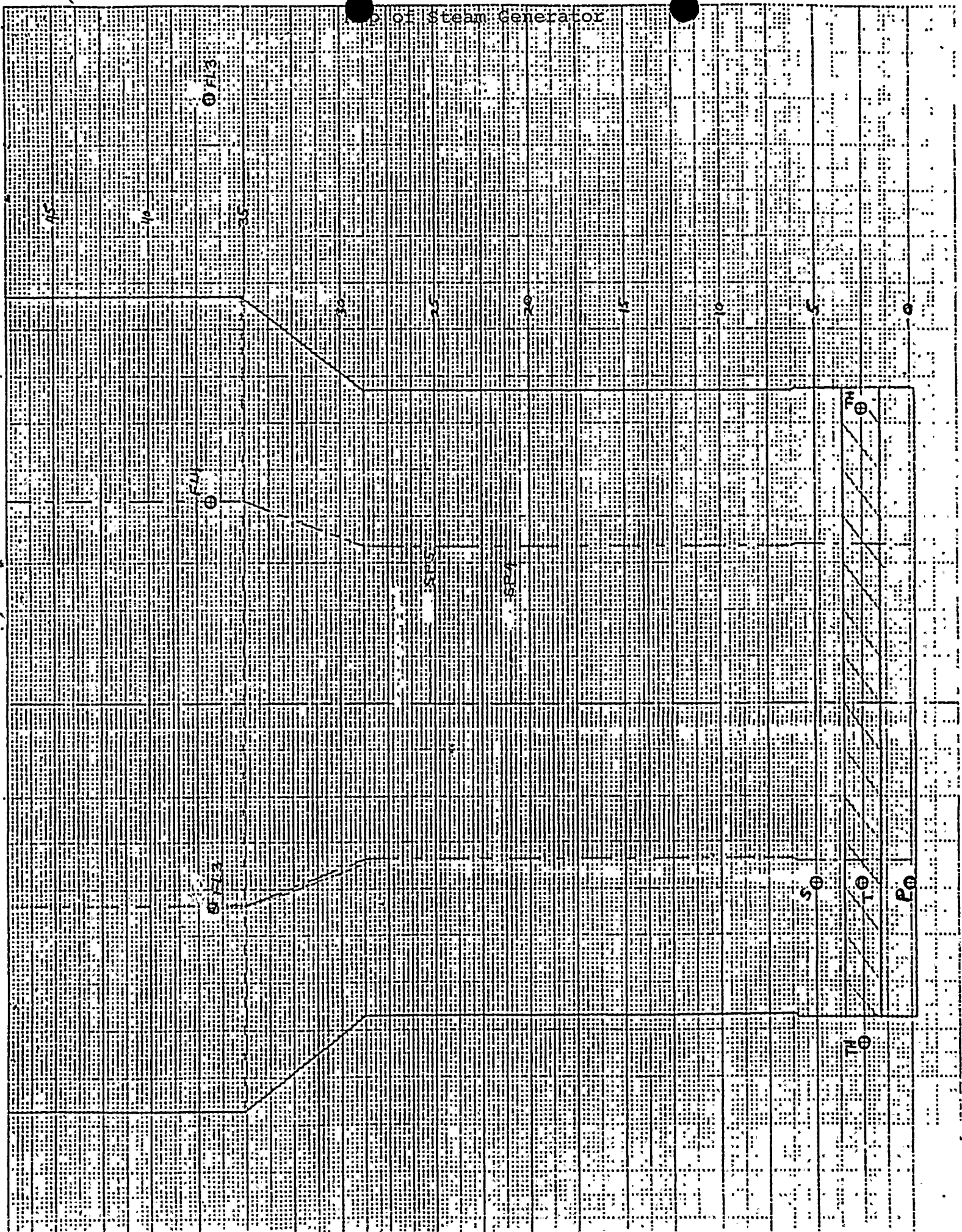




Figure 2.

Top of Steam Generator





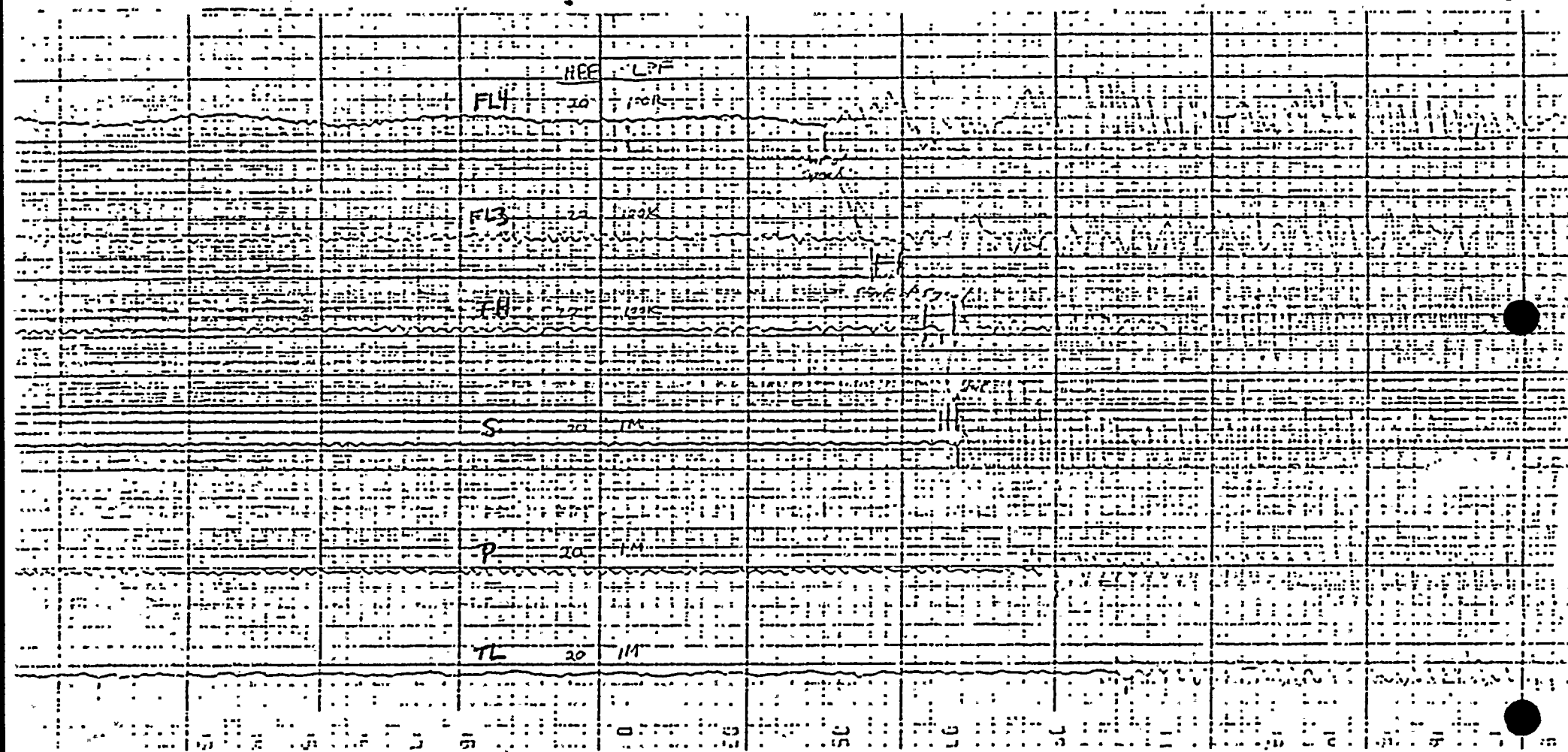


Figure 3. Visicorder Time Trace of RGE Tape 008 274 Ft.  
One Time Division Equals 62.5 Microseconds

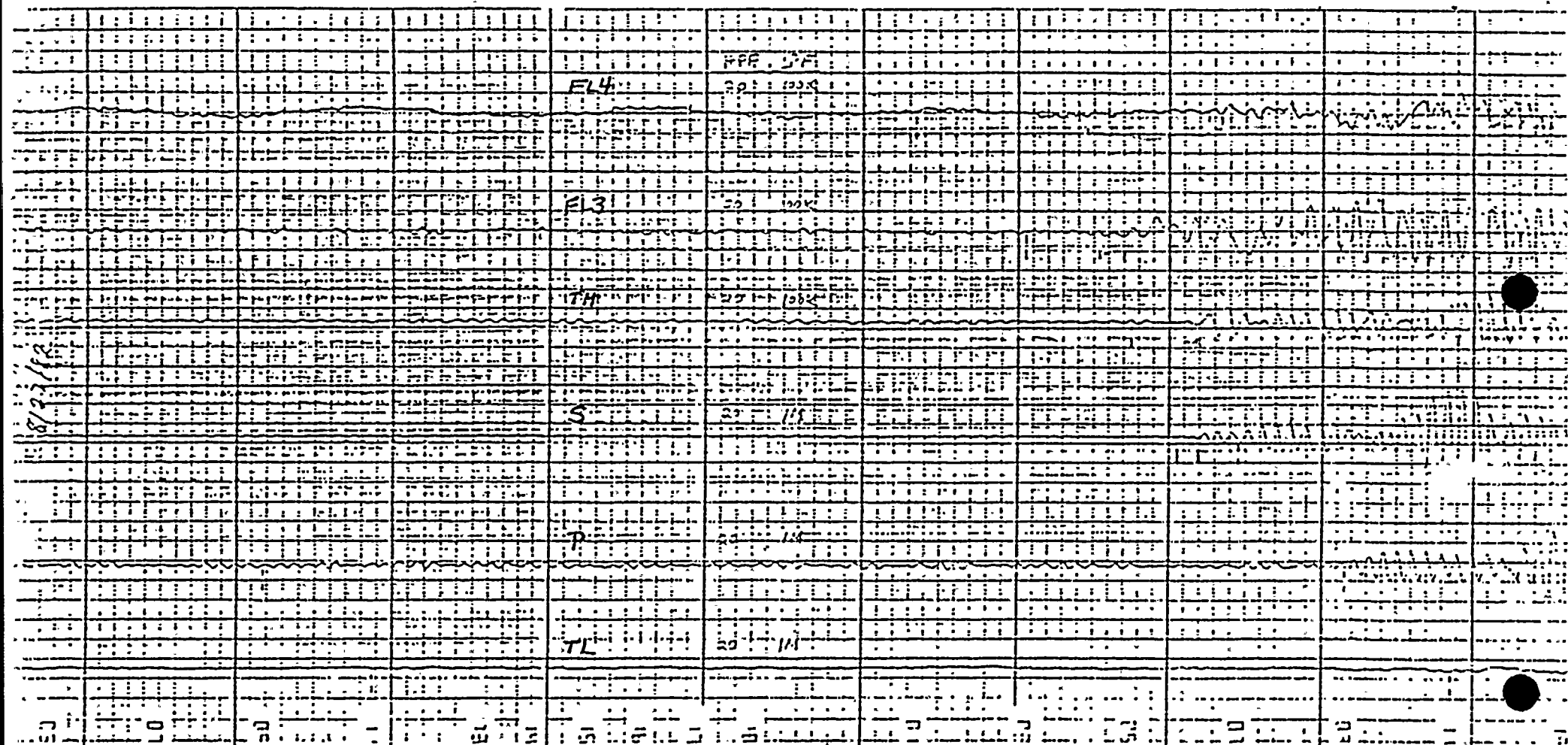


Figure 4. Visicorder Time Trace of RGE Tape 008 400 Ft.  
One Time Division Equals 62.5 Microseconds









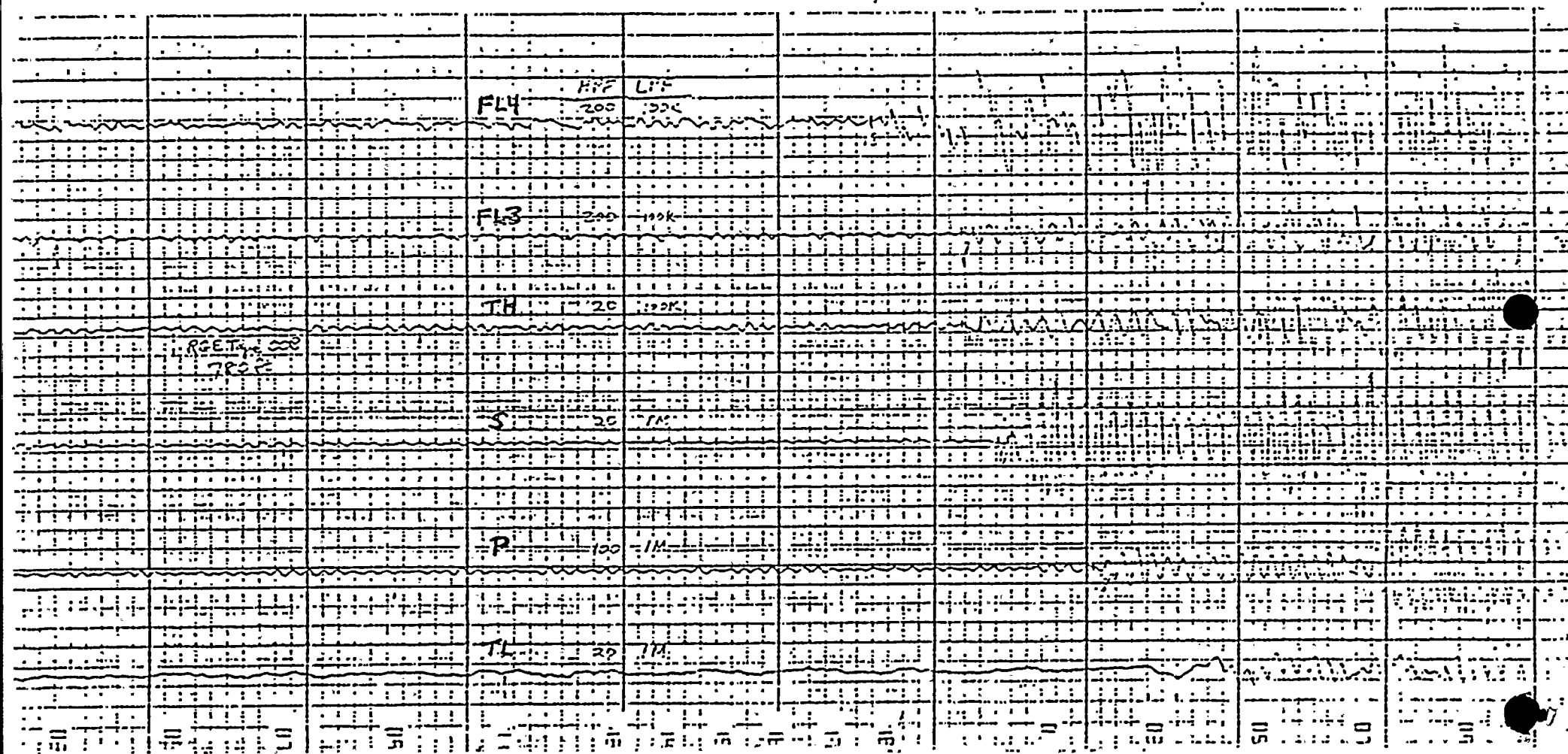


Figure 6. Visicorder Time Trace of RGE Tape 008 780 Ft.  
One Time Division Equals 62.5 Microseconds .



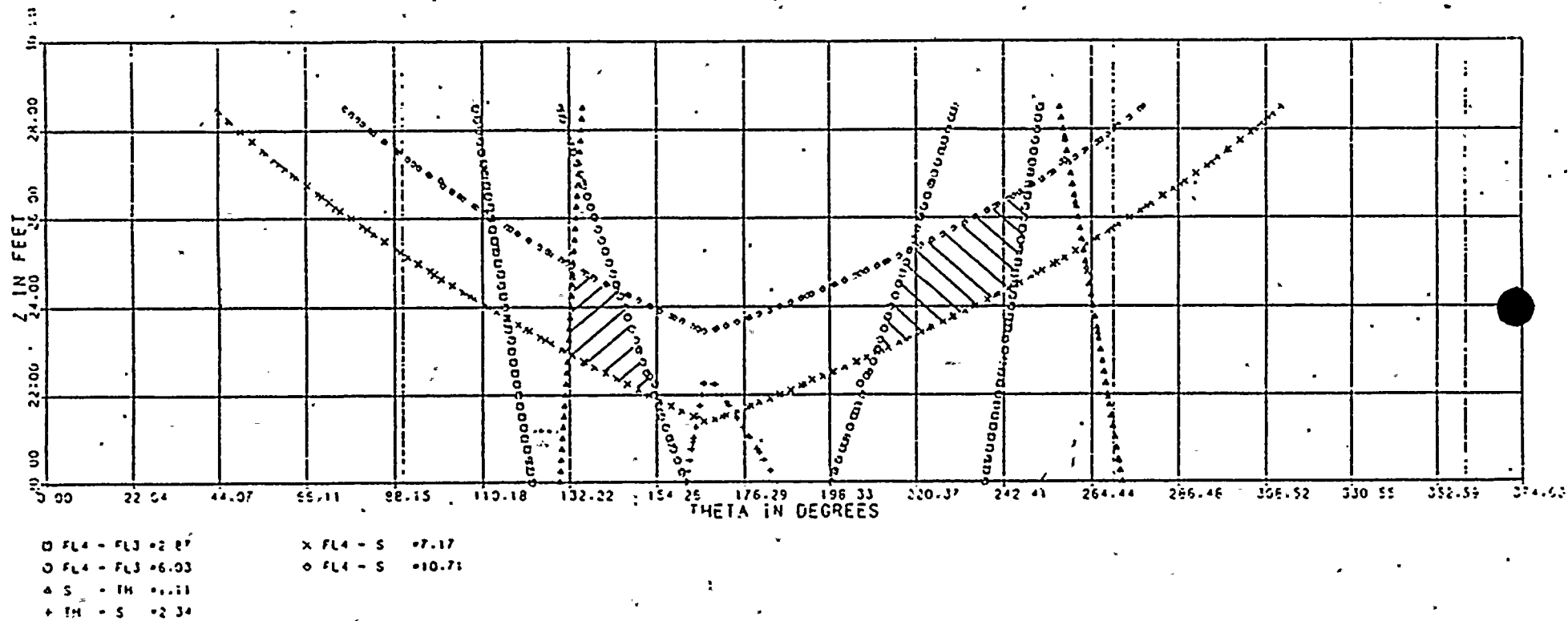


Figure 7. Triangulation Plot of Tape RGE 008 274 Ft.  
Maximum Error Bounds



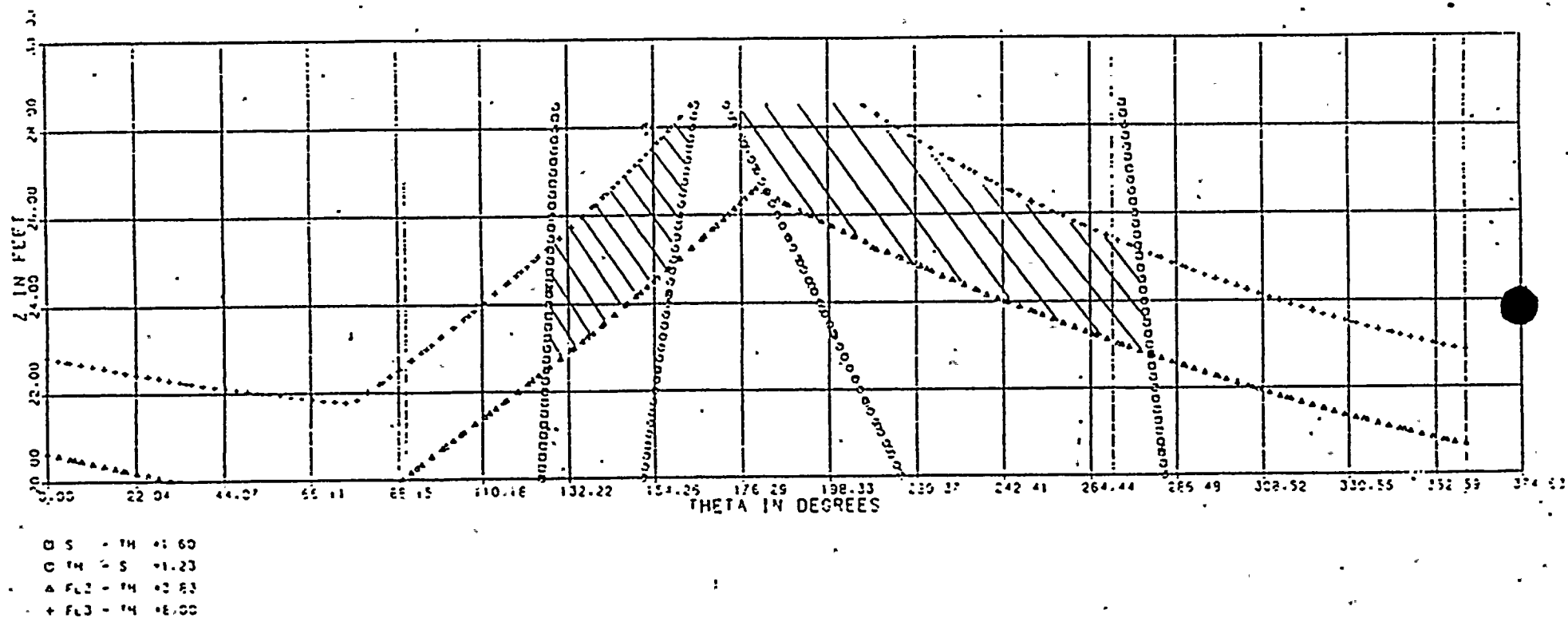


Figure 8. Triangulation Plot of Tape RGE 008 400 Ft.  
Maximum Error Bounds





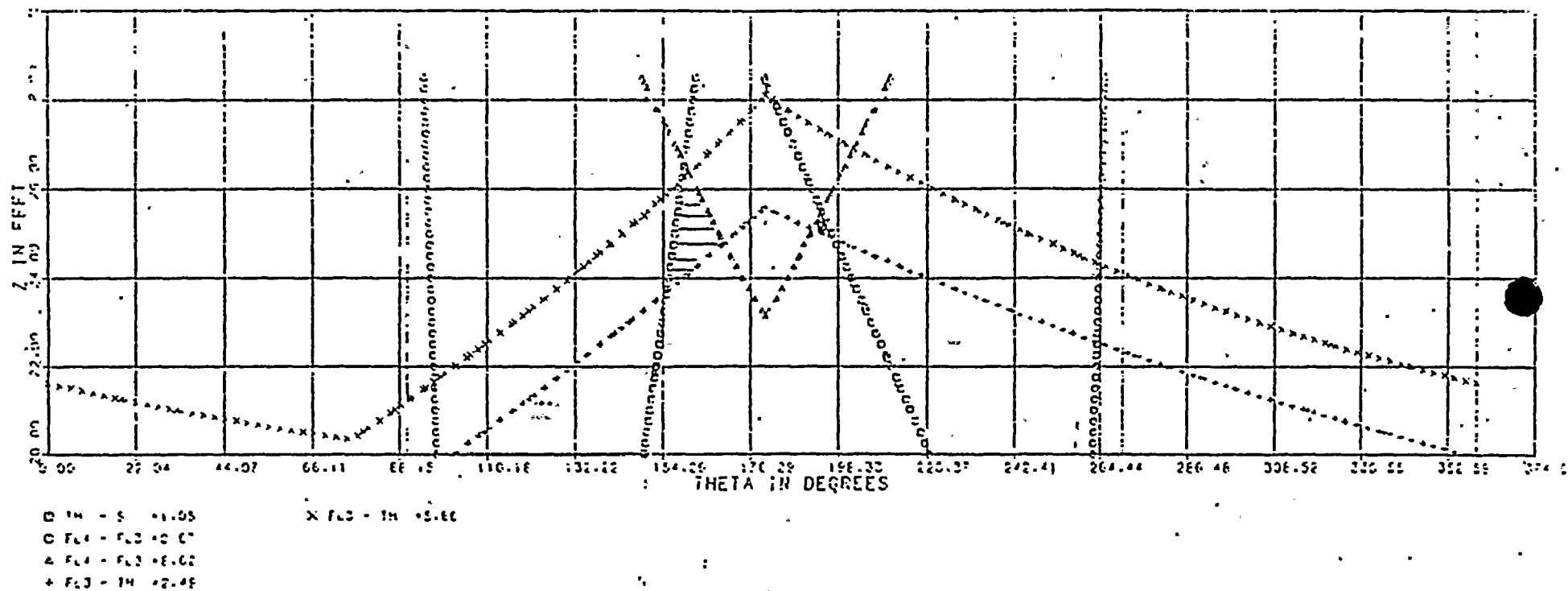
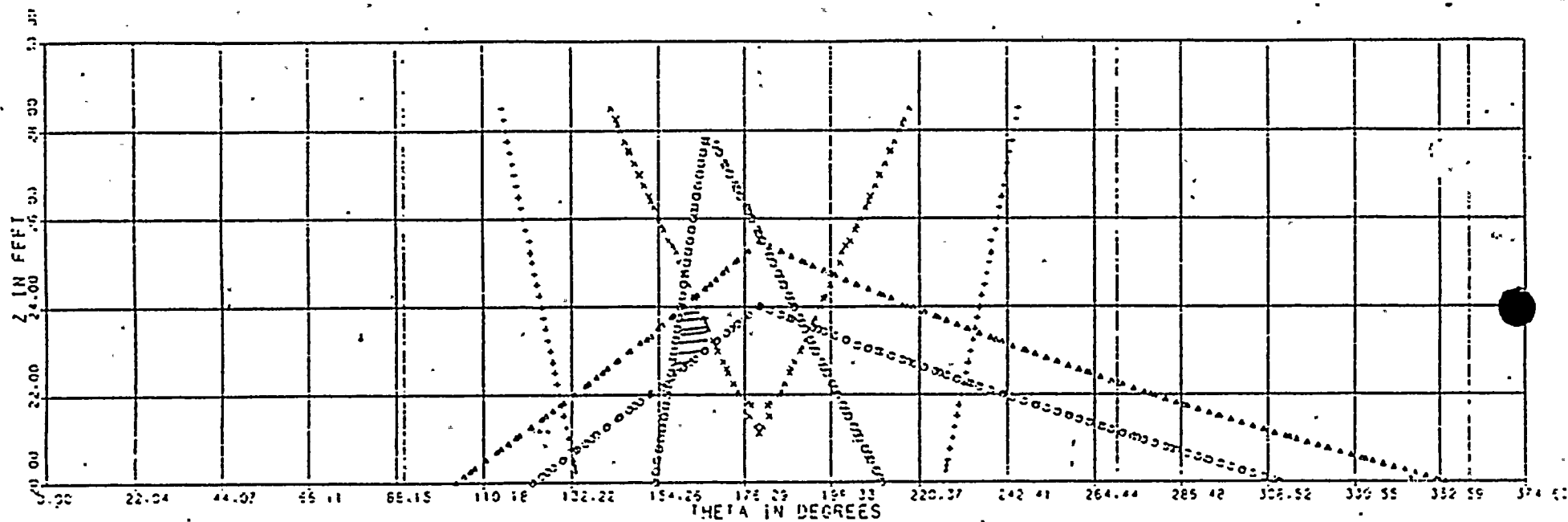


Figure 9. Triangulation Plot of Tape RGE 008 680 Ft.  
Maximum Error Bounds





O 14 - 5 - 1.42  
 O FL3 - 14 - 0.29  
 A FL3 - 14 - 2.34  
 + FL4 - FL3 - 3.83

X FL4 - FL3 - 7.16

Figure 10. Triangulation Plot of Tape RGE 008 780 Ft  
 Maximum Error Bounds



NEI94.,120

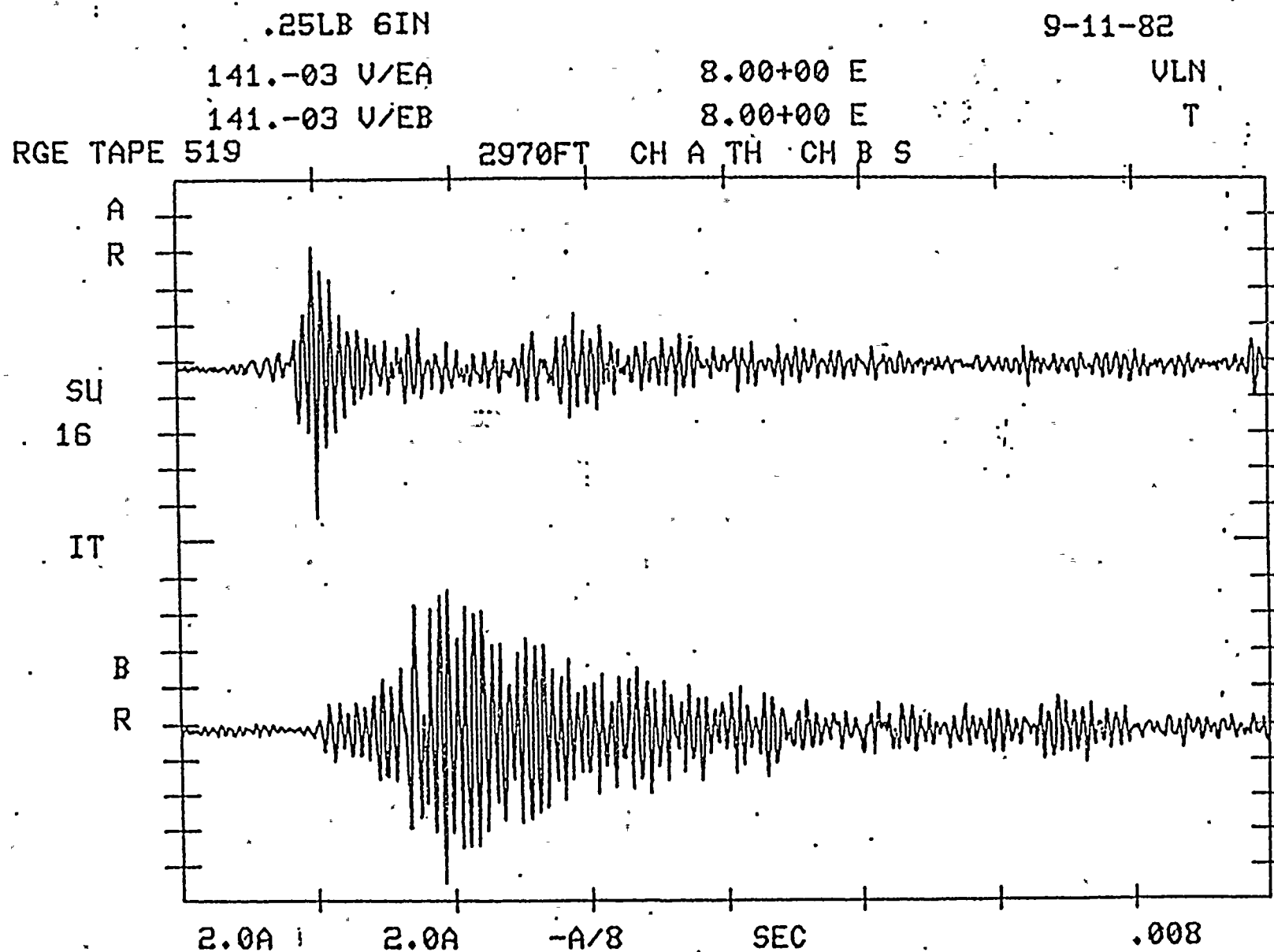


Figure 11A. Time Trace of Simulated Impact  
.25 LB. 6 In. Drop



NEI94.,120

.25LB 6IN

9-11-82

141.-03 V/EA

300.-03 E

VLN

141.-03 V/EB

800.-03 E

T

RGE TAPE 519

2910-3052 CHA TH CH B S

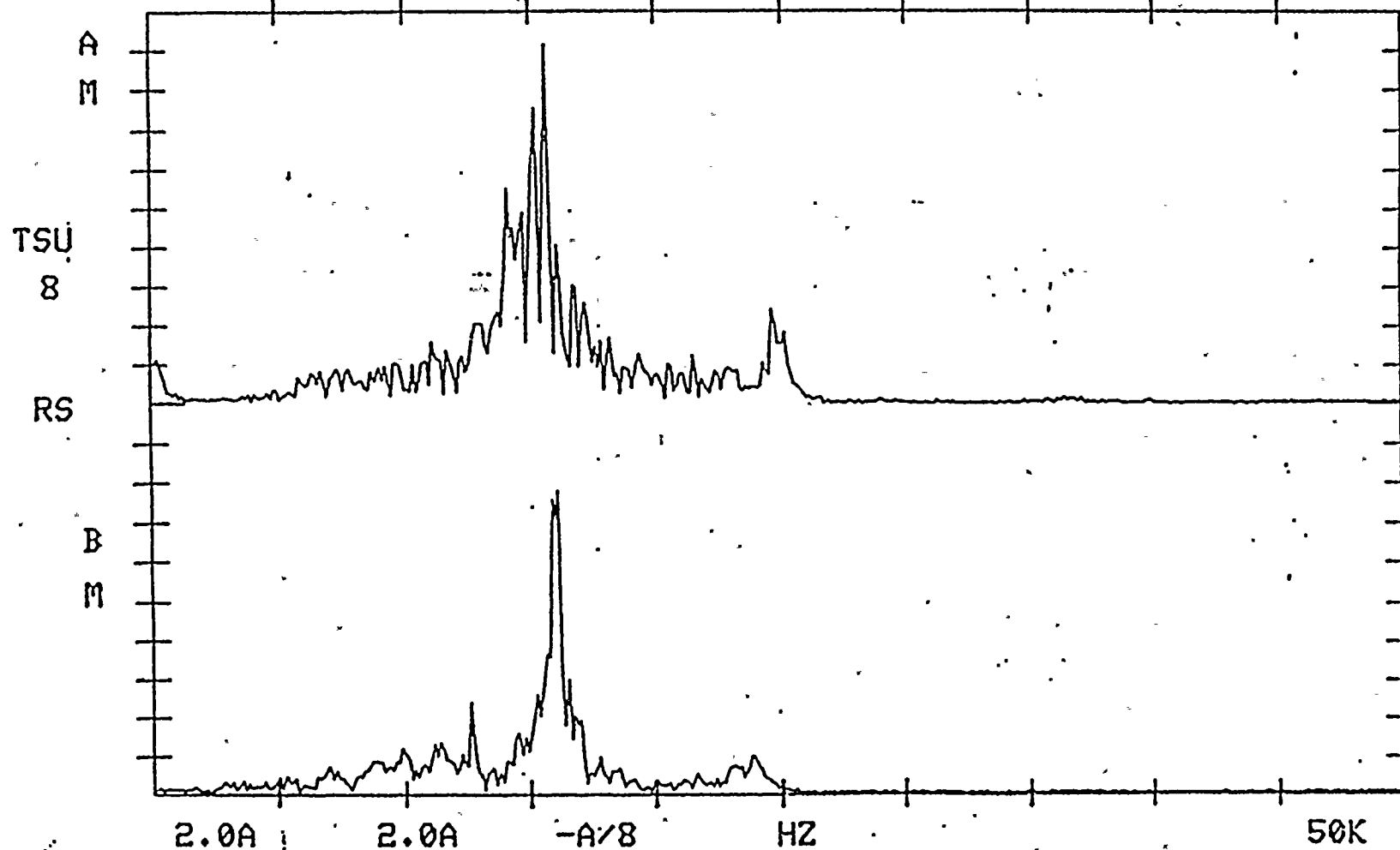


Figure 11B. Frequency Spectrum of Simulated Impact  
.25 Lb. 6 In. Drop





NEI94.,120

.5LB 6IN

9-11-82

~~141.-03~~ V/EA

~~8.00+00~~ E

VLN

141.-03 V/EB

8.00+00 E

T

RGE TAPE 519

2020FT

CH A TH

CH B S

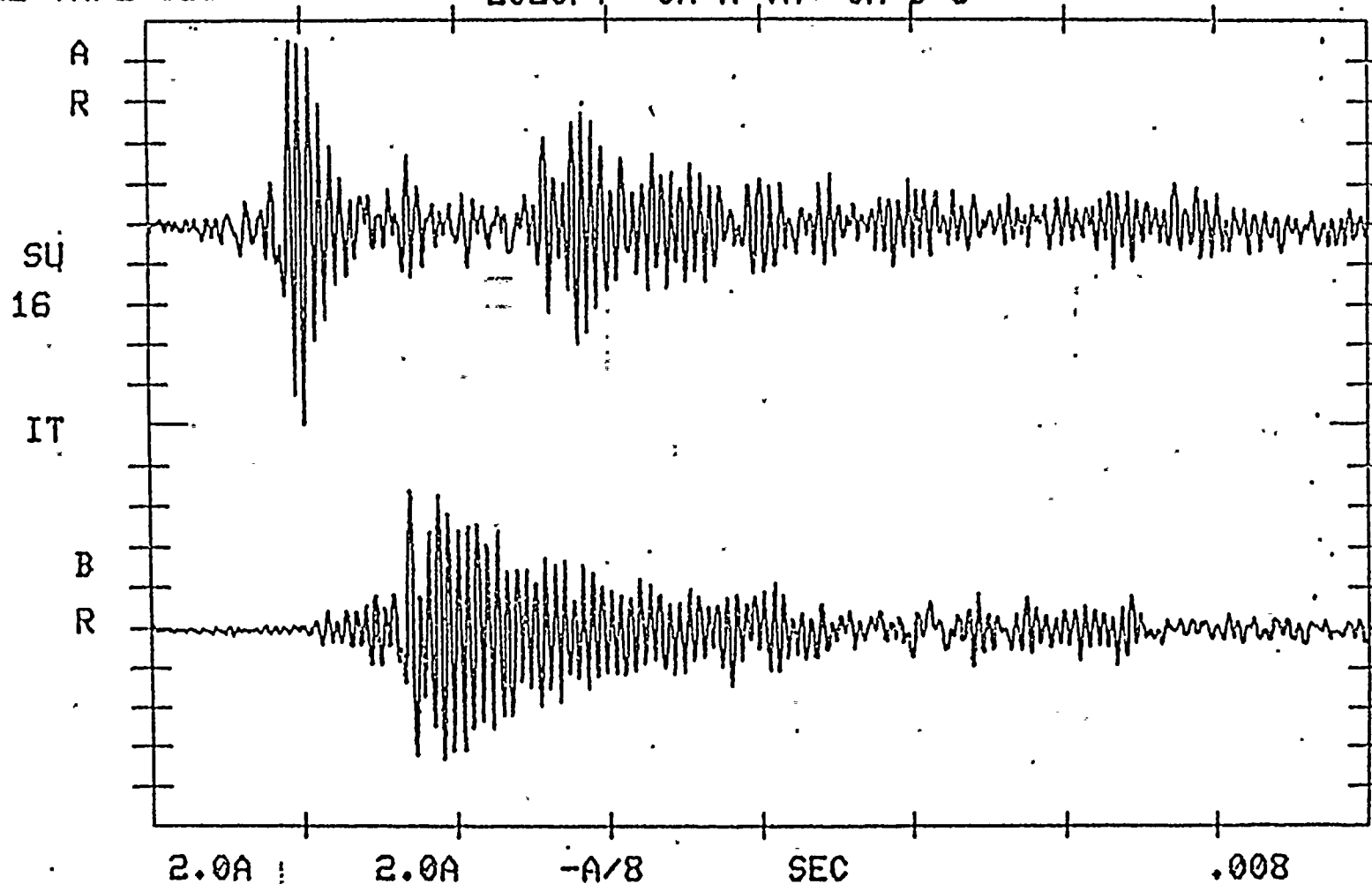


Figure 12A. Time Trace of Simulated Impact  
.5 LB. 6 In. Drop



NEI94.,120

*should be*  
470 .5LB 6IN  
~~141~~ -03 V/EA  
141.-03 V/EB

*500 as shown*  
~~500~~ -03 E  
500.-03 E

9-11-82

VLN  
T

RGE TAPE 519

2000-2147 CHA TH CH B S

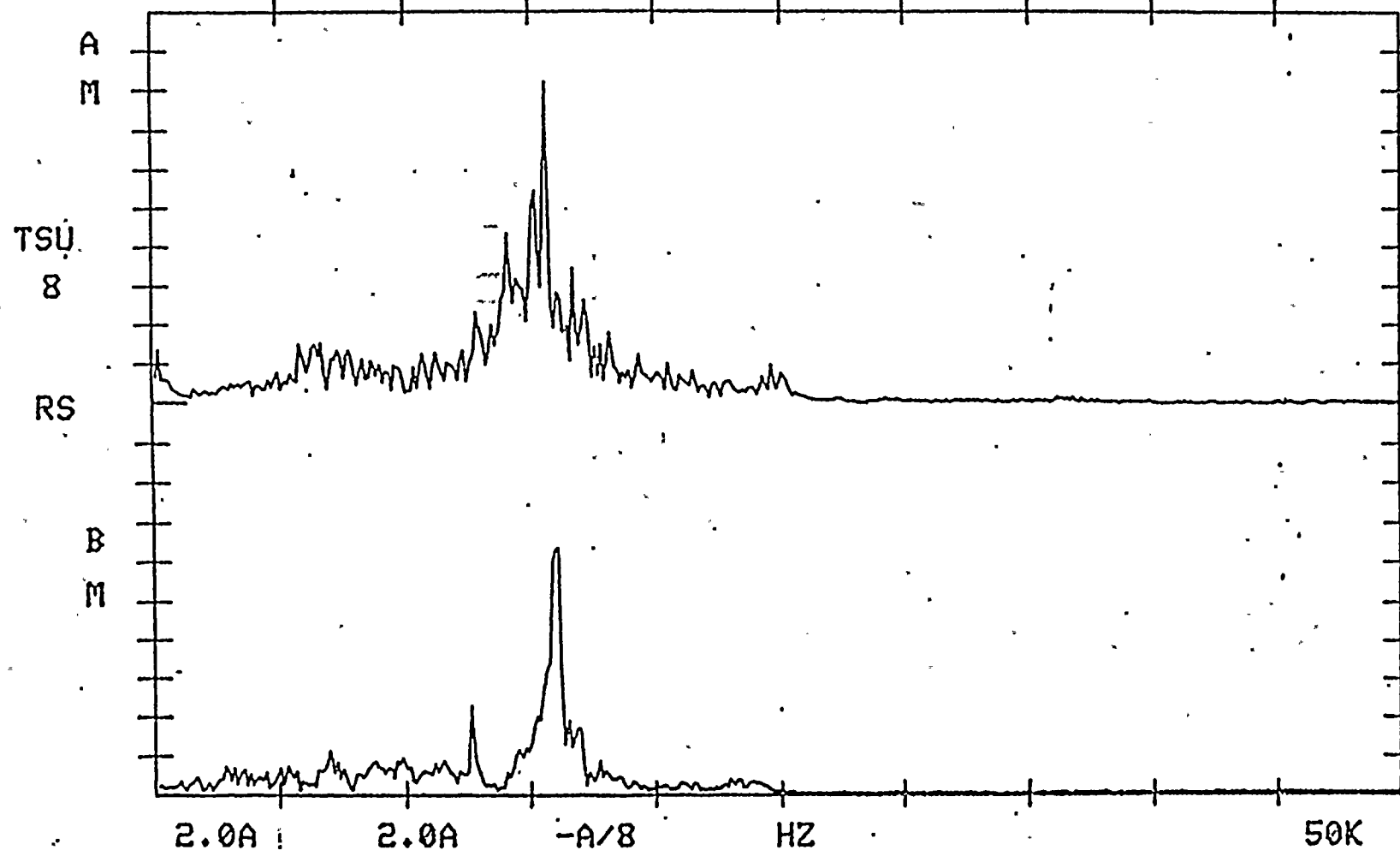


Figure 12B. Frequency Spectrum of Simulated Impact  
.5 Lb. 6 In. Drop

NEI94.,120

1LB 6IN

9-11-82

141.-03 U/EA

5.00+00 E

VLN

141.-03 U/EB

5.00+00 E

T

RGE TAPE 519

1380FT

CH A TH

CH B S

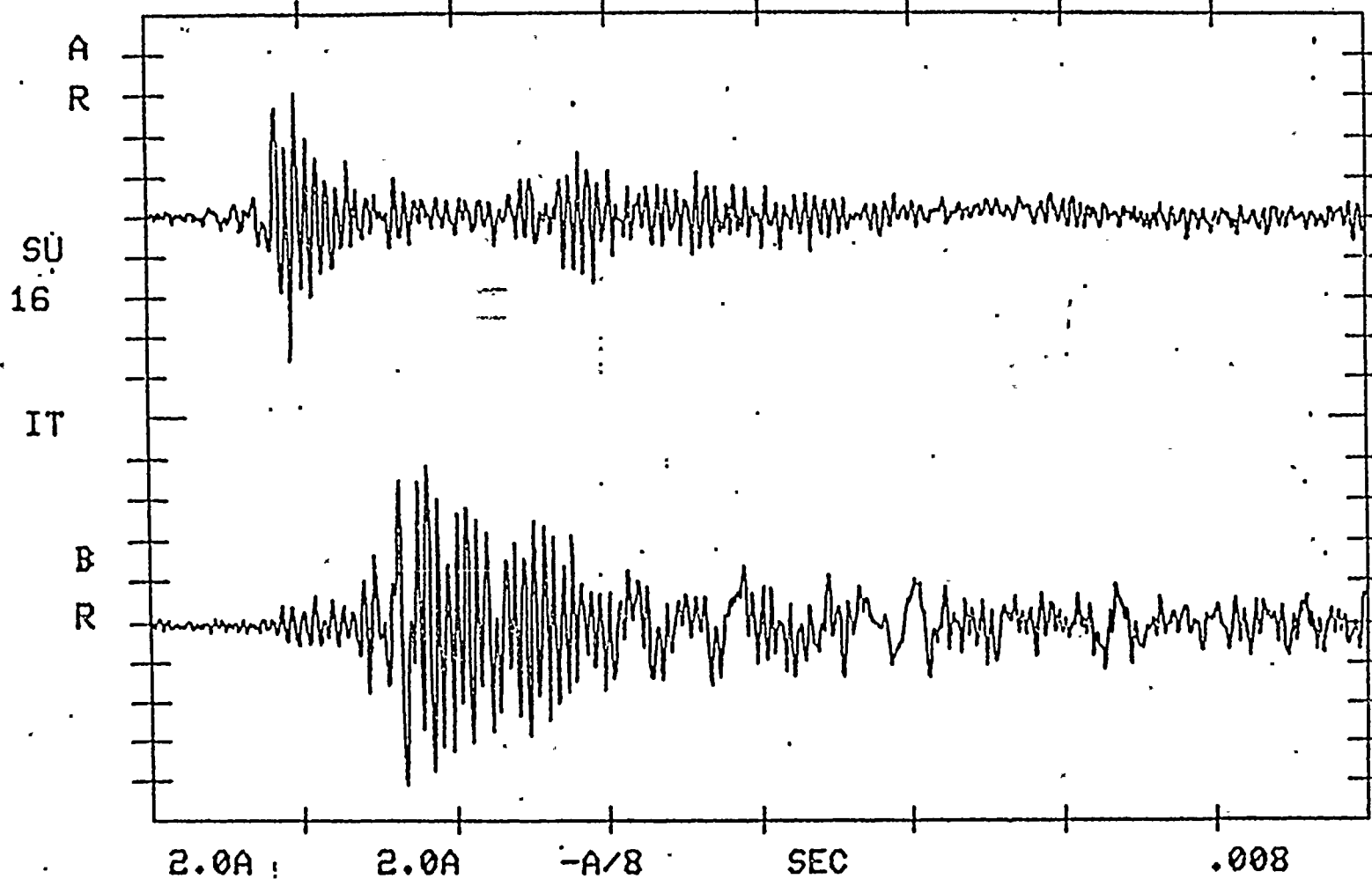


Figure 13A. Time Trace of Simulated Impact  
1.0 LB. 6 In. Drop

NEI94.,120

1LB 6IN

9-11-82

141.-03 V/EA

200.-03 E

VLN

141.-03 V/EB

500.-03 E

T

RGE TAPE 519

1245-1412 CHA TH CH B S

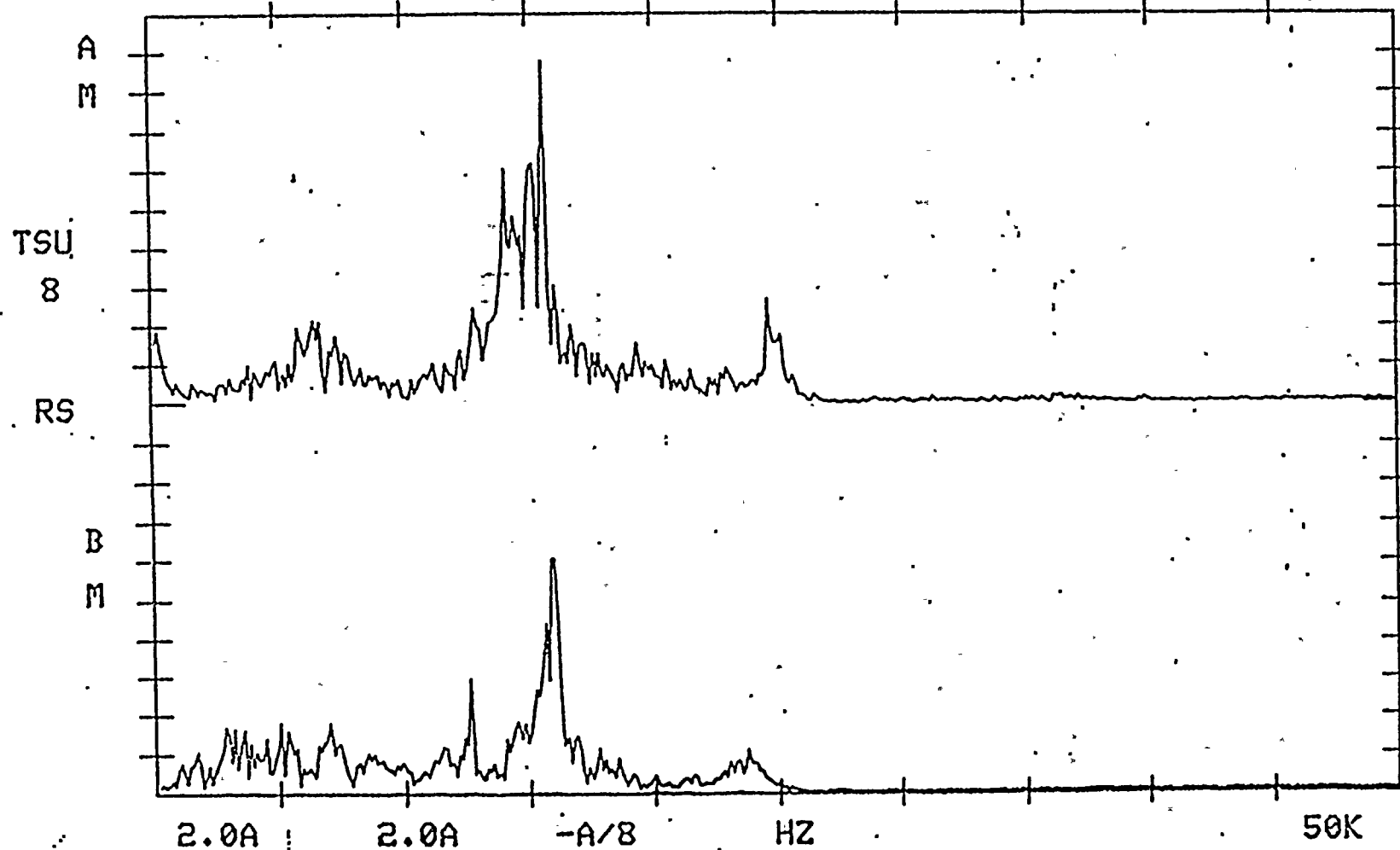


Figure 13B. Frequency Spectrum of Simulated Impact  
1.0 Lb. 6 In. Drop



NEI94.,120

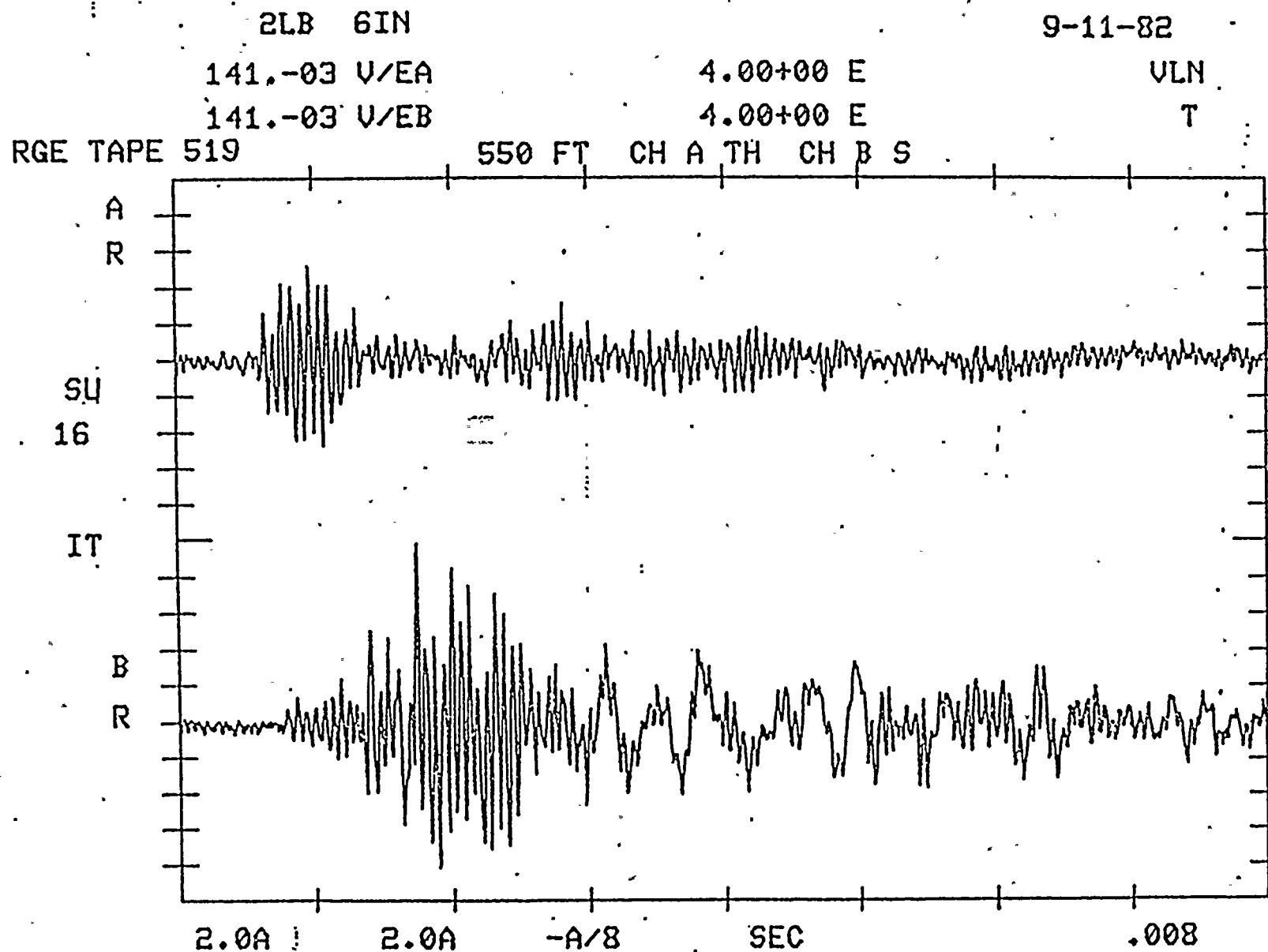


Figure 14A. Time Trace of Simulated Impact  
2.0 LB. 6 In. Drop





NEI94.,120

2LB .6IN

9-11-82

141.-03 V/EA

200.-03 E

VLN

141.-03 V/EB

500.-03 E

T

RGE TAPE 519

490-690FT CHA TH CH B S

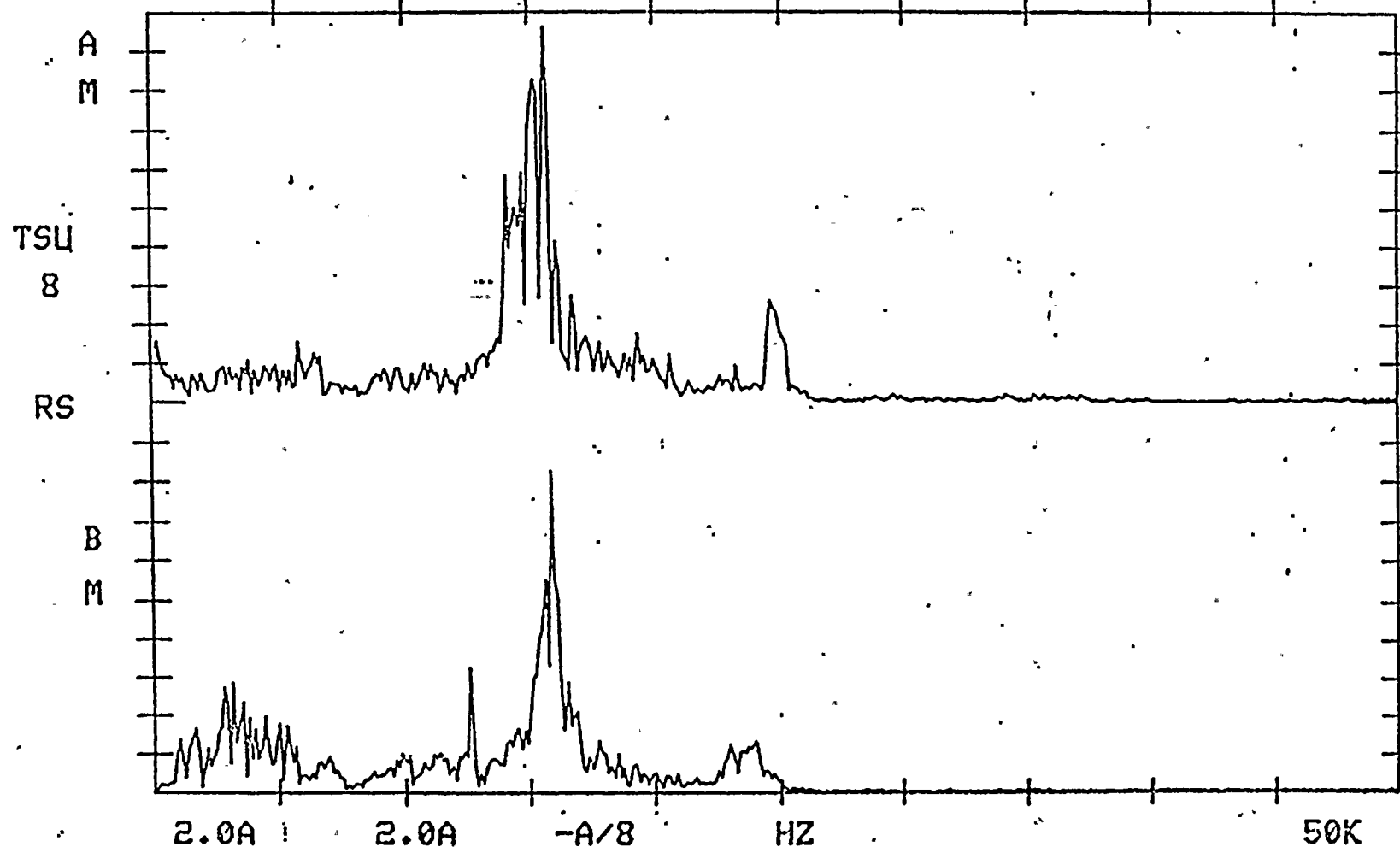
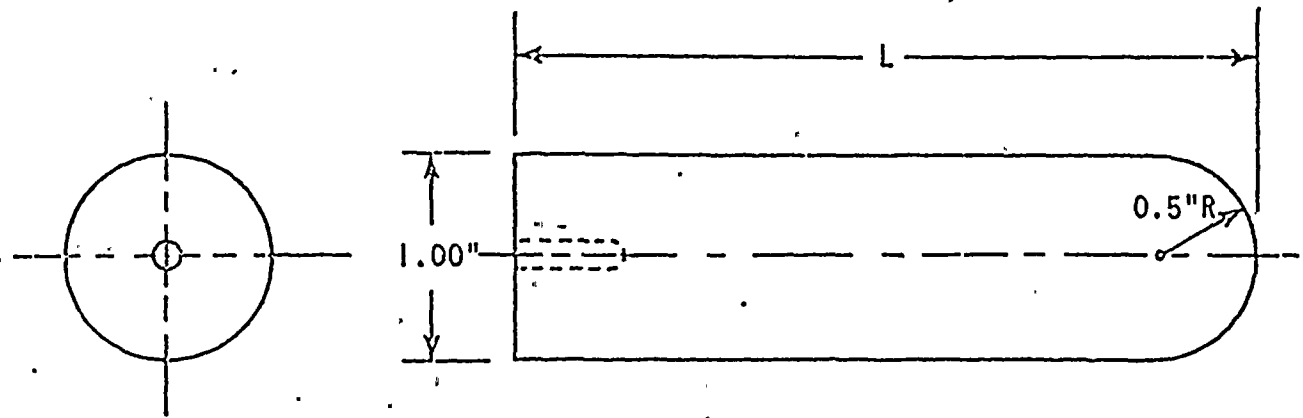


Figure 14B. Frequency Spectrum of Simulated Impact  
2.0 Lb. 6 In. Drop





LENGTH (L)	TOTAL WEIGHT
(IN.)	(LB)
13.65	3.0
11.40	2.5
9.16	2.0
6.91	1.5
4.66	1.0
2.41	0.5
1.29	0.25

MATERIAL: 304 STAINLESS STEEL

Figure 15. Steel Rods Used in Metal Impact Simulation Experiments



NEI94.,120

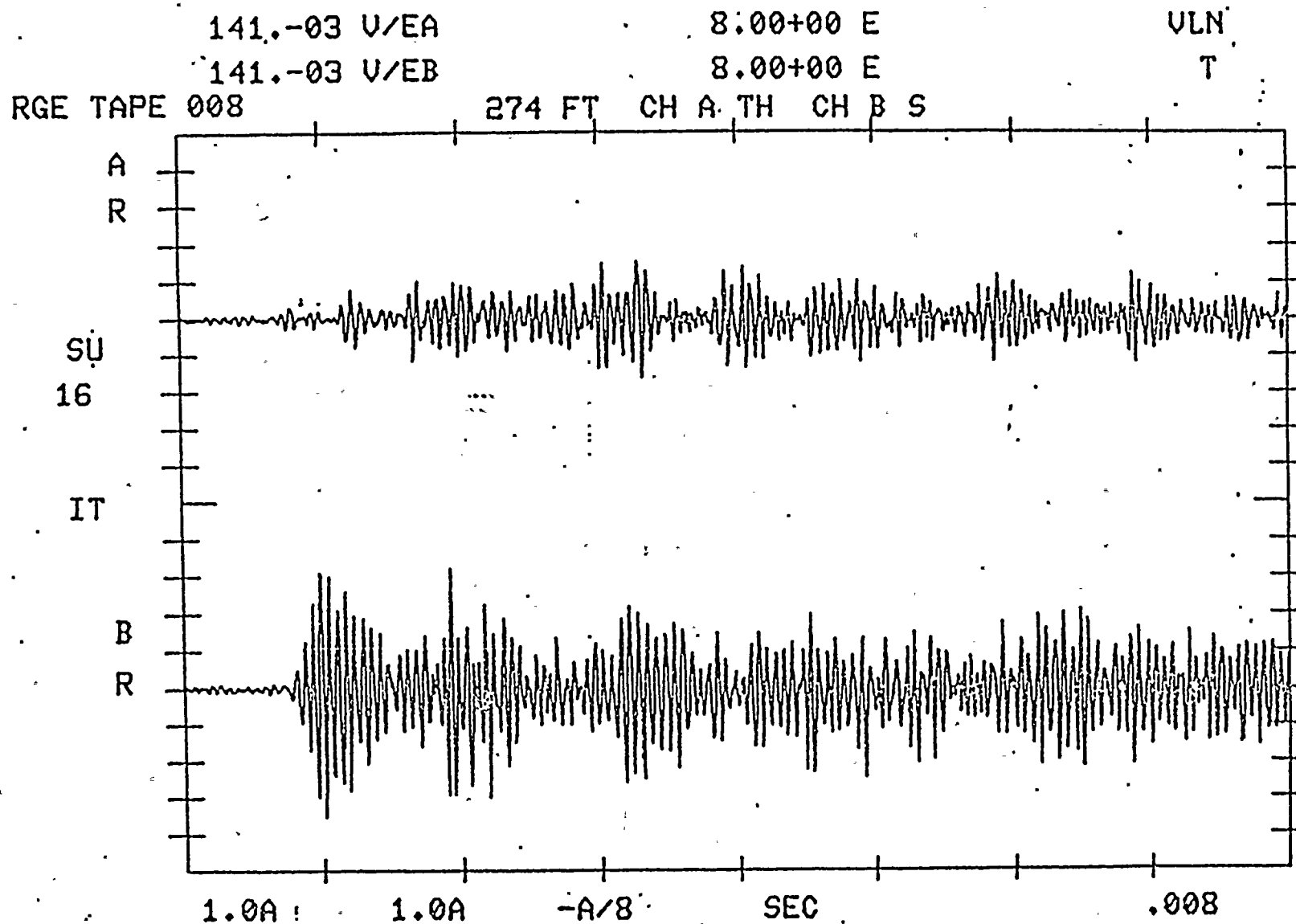


Figure 16A. Time Trace of Real Impact  
Tape RGE 008 274 Ft.



100

NEI94.,120

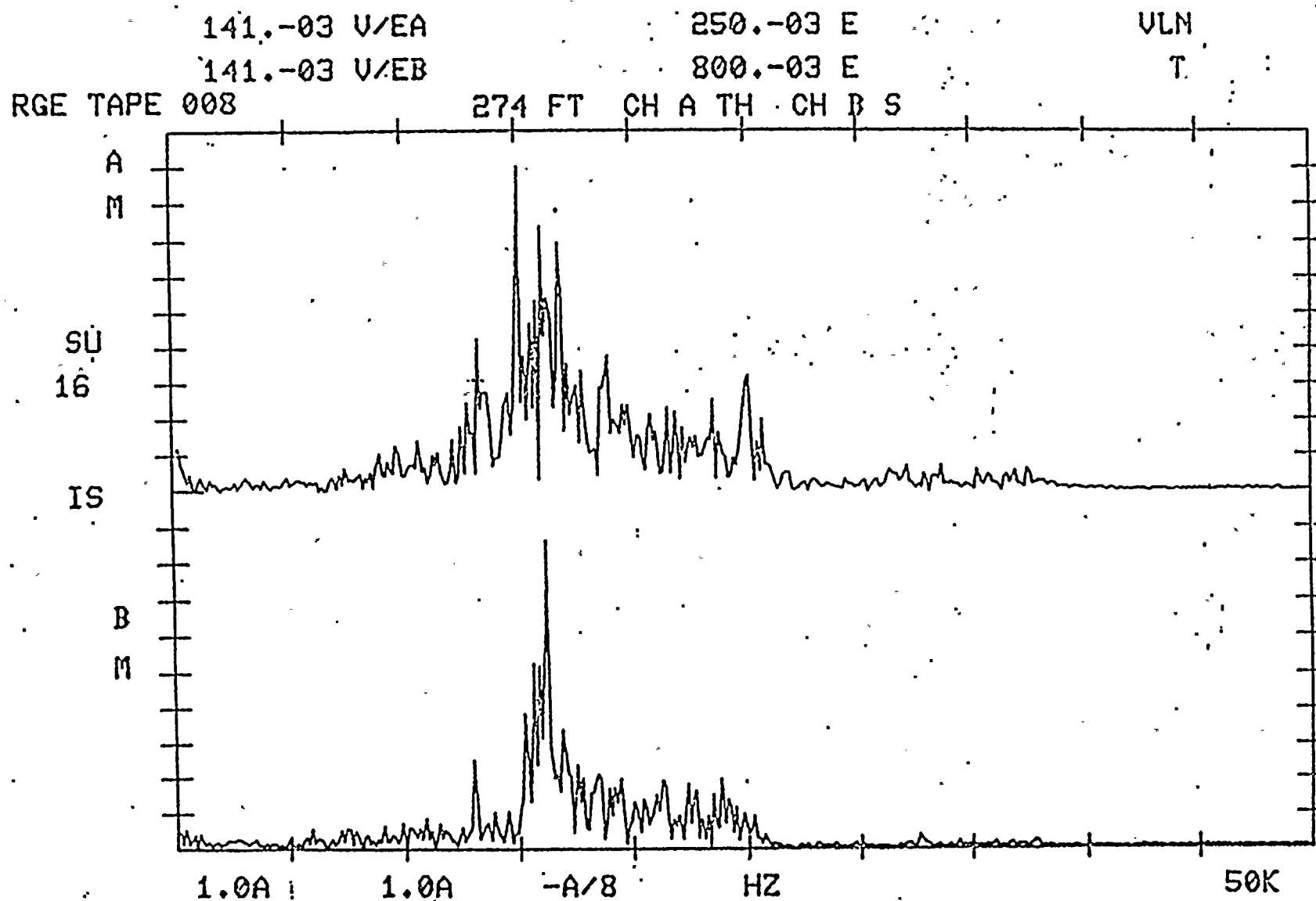


Figure 16B. Frequency Spectrum of Real Impact  
Tape RGE 008 274 Ft.





NEI94.,120

9-11-82

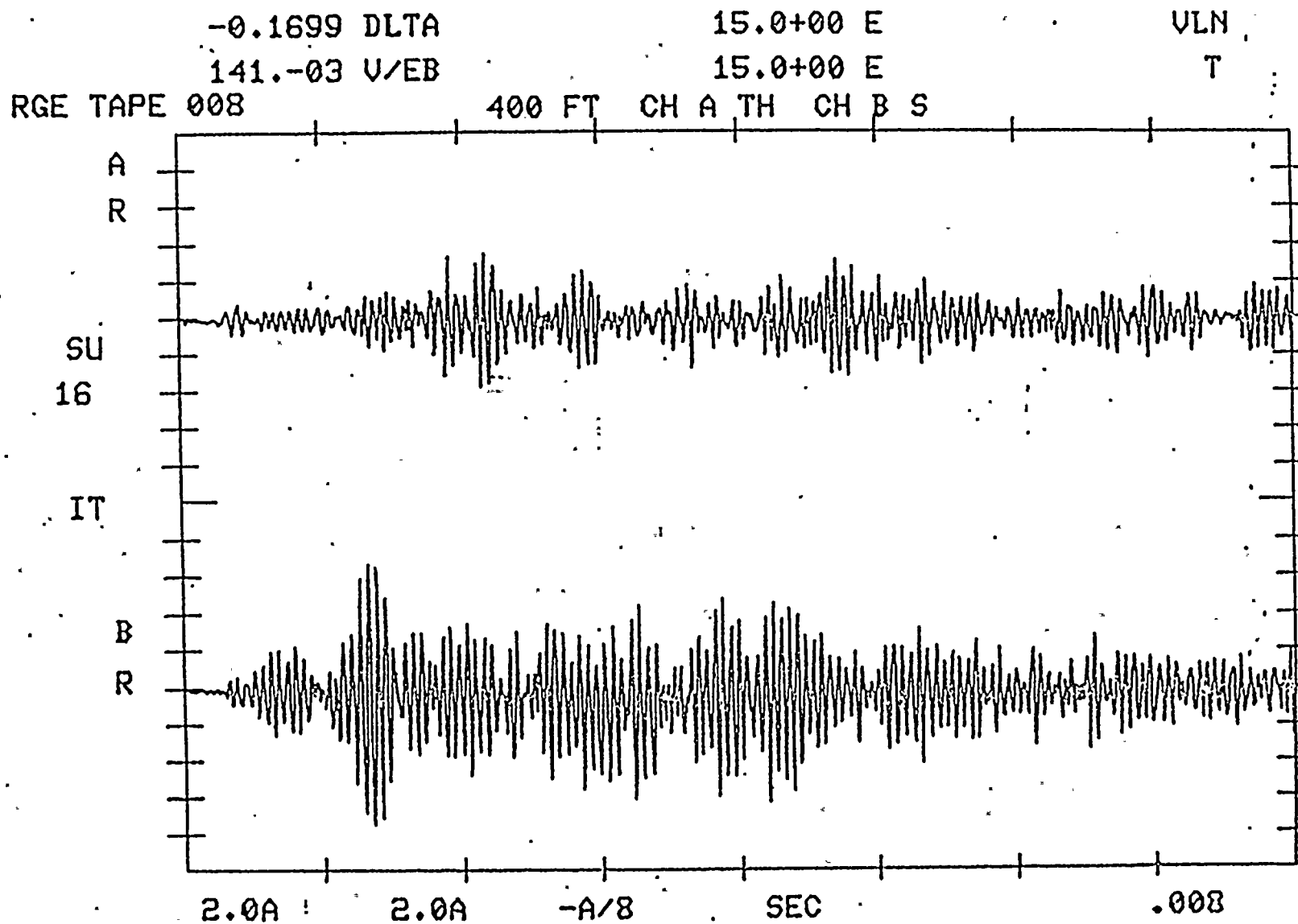


Figure 17A. Time Trace of Real Impact  
Tape RGE 008 400 Ft.



NEI94.,120

9-11-82

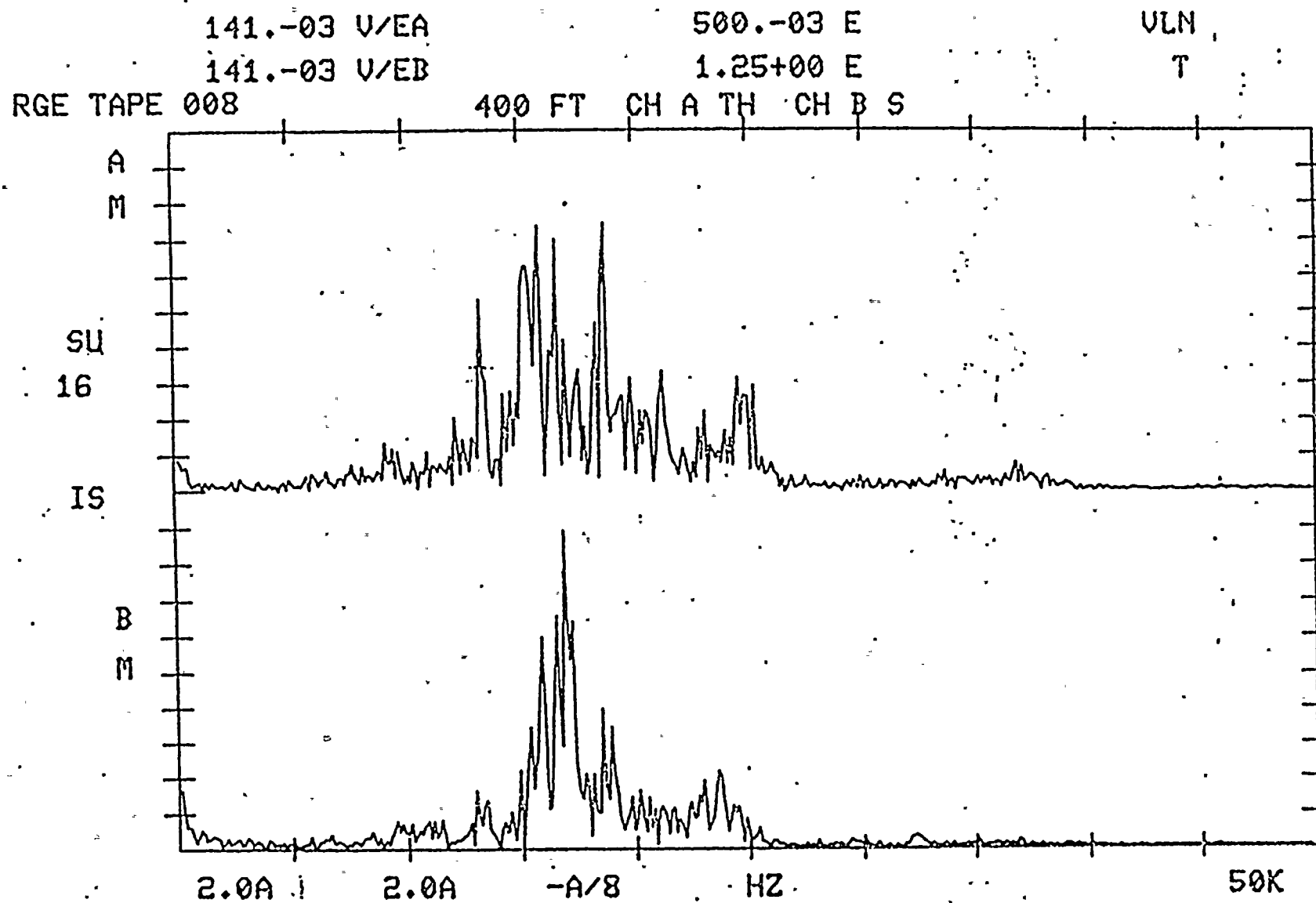


Figure 17B. Frequency Spectrum of Real Impact  
Tape RGE 008 400 Ft.



11

NEI94.,120

9-11-82

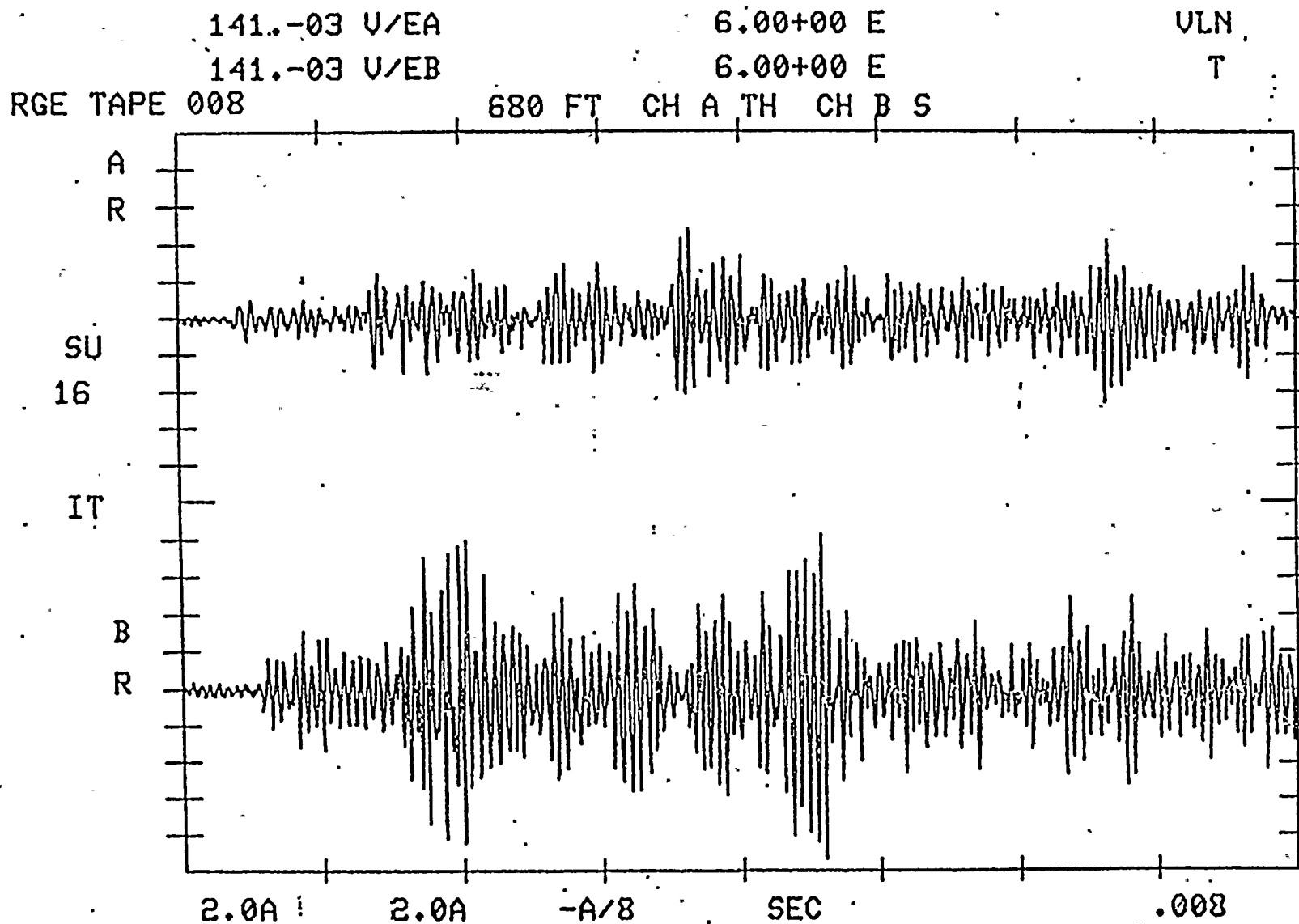


Figure 18A. Time Trace of Real Impact  
Tape RGE 008 680 Ft.



NEI94.,120

9-11-82

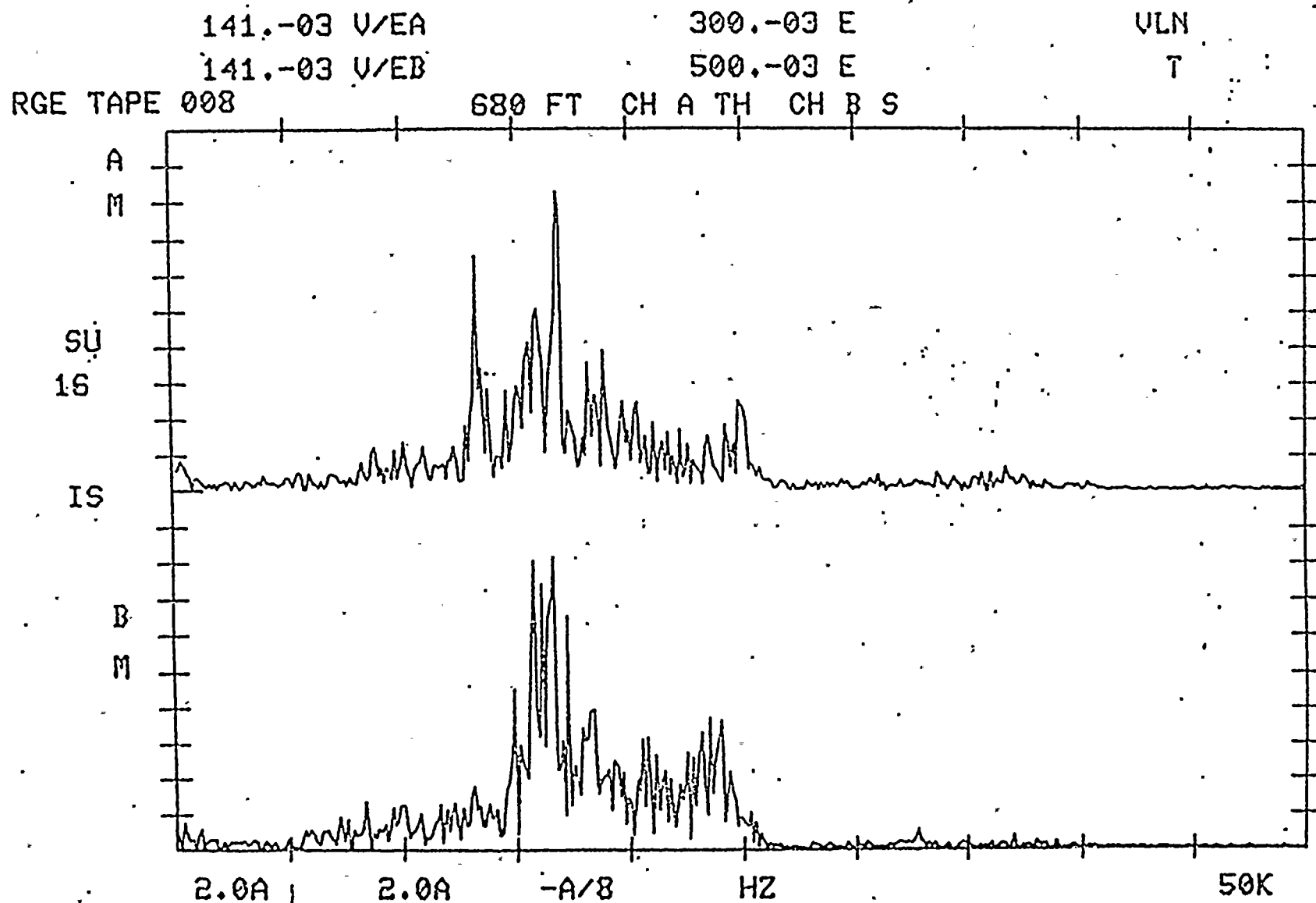


Figure 18B. Frequency Spectrum of Real Impact  
Tape: RGE 008 680 Ft.





NEI94.,120

9-11-82

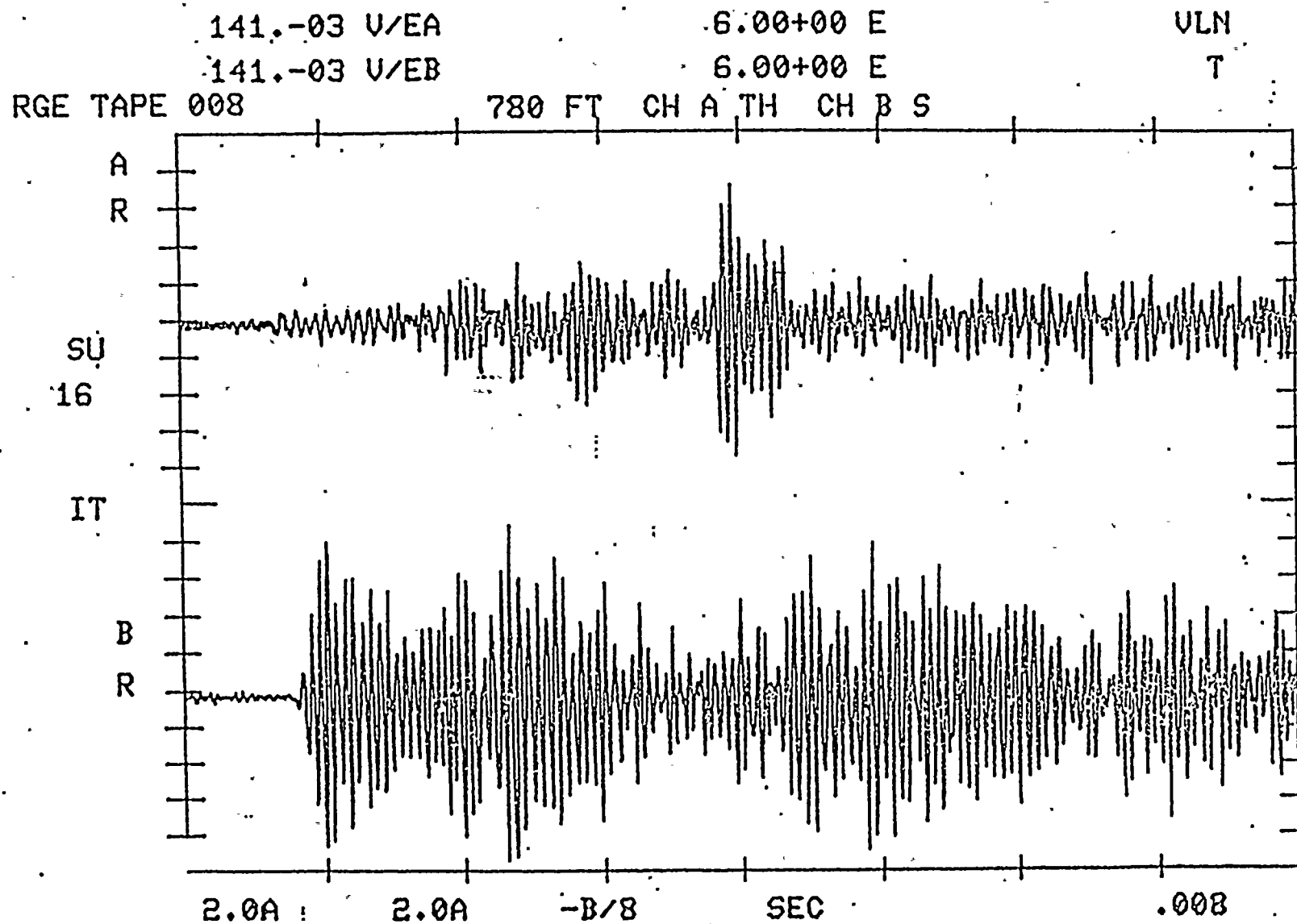


Figure 19A. Time Trace of Real Impact  
Tape RGE 008 780 Ft.



NEI94.,120

9-11-82

141.-03 V/EA

300.-03 E

VLN

141.-03 V/EB

800.-03 E

T

RGE TAPE 008

780 FT

CH A TH

CH B S

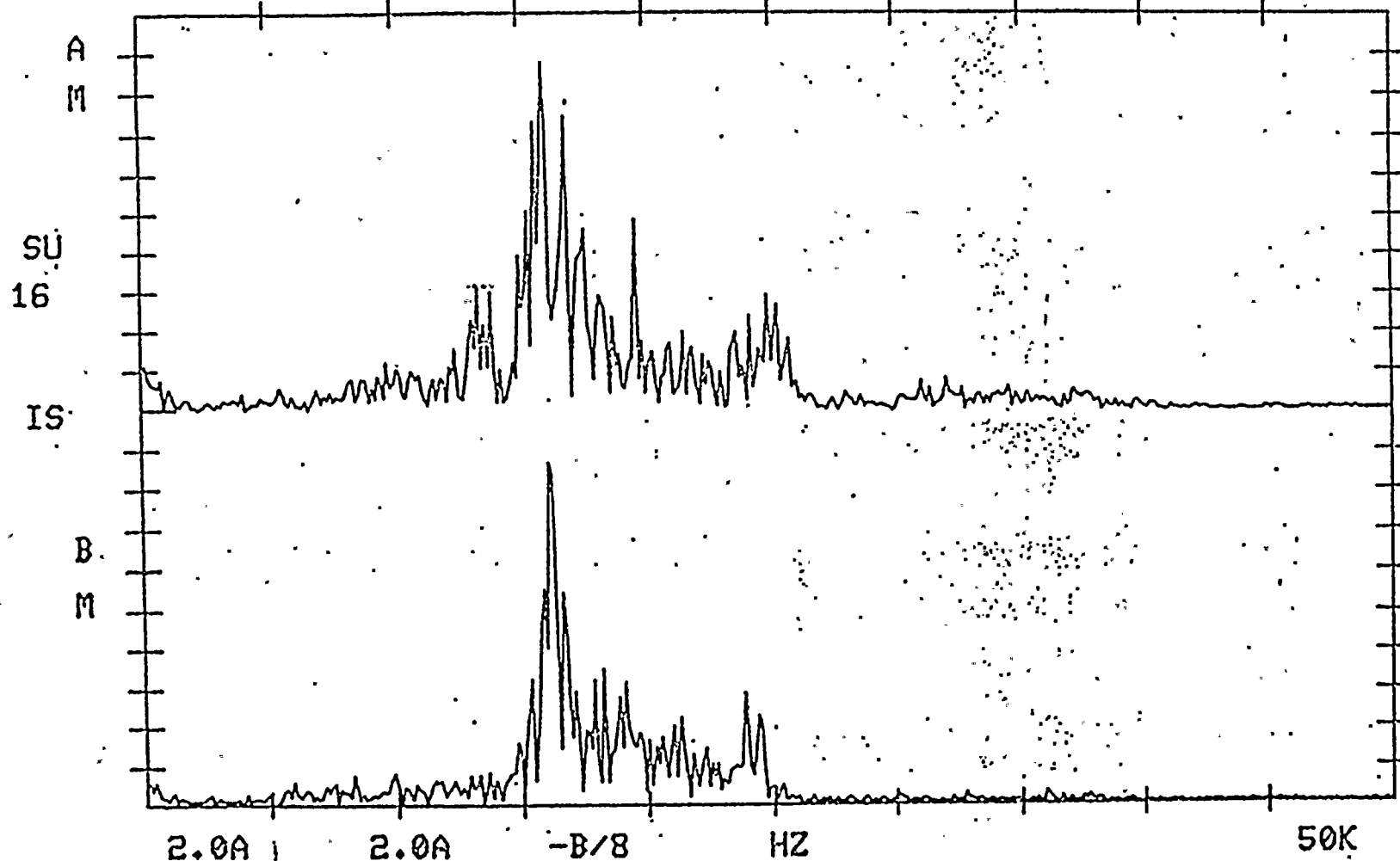


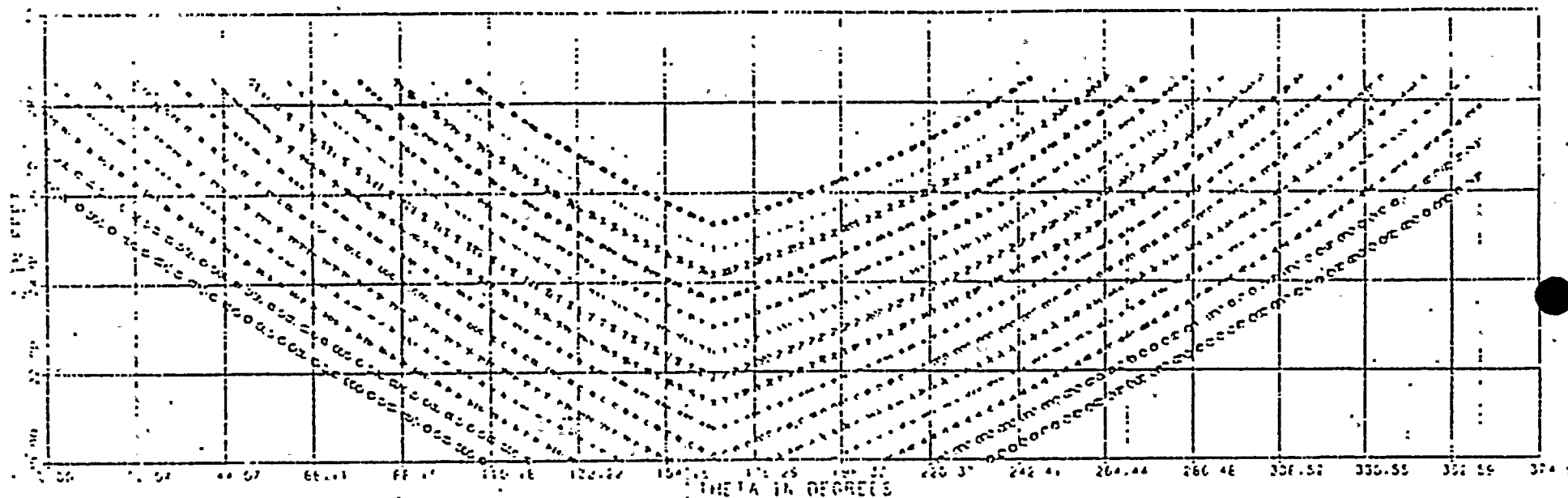
Figure 19B. Frequency Spectrum of Real Impact  
Tape RGE 008 780 Ft.



## APPENDIX

Figures A1 to A4 provide families of constant distance-difference curves for the four sensors used in this analysis.





0 FL4 - S	+0.00	8 FL4 - S	+8.00	16 FL4 - S	+16.00	24 FL4 - S	+24.00
1 FL4 - S	+1.00	9 FL4 - S	+9.00	17 FL4 - S	+17.00	25 FL4 - S	+25.00
2 FL4 - S	+2.00	10 FL4 - S	+10.00	18 FL4 - S	+18.00	26 FL4 - S	+26.00
3 FL4 - S	+3.00	11 FL4 - S	+11.00	19 FL4 - S	+19.00	27 FL4 - S	+27.00
4 FL4 - S	+4.00	12 FL4 - S	+12.00	20 FL4 - S	+20.00	28 FL4 - S	+28.00
5 FL4 - S	+5.00	13 FL4 - S	+13.00	21 FL4 - S	+21.00	29 FL4 - S	+29.00
6 FL4 - S	+6.00	14 FL4 - S	+14.00	22 FL4 - S	+22.00	30 FL4 - S	+30.00
7 FL4 - S	+7.00	15 FL4 - S	+15.00	23 FL4 - S	+23.00	31 FL4 - S	+31.00

Figure A1. Family of FL4-S Distance-Difference Curves





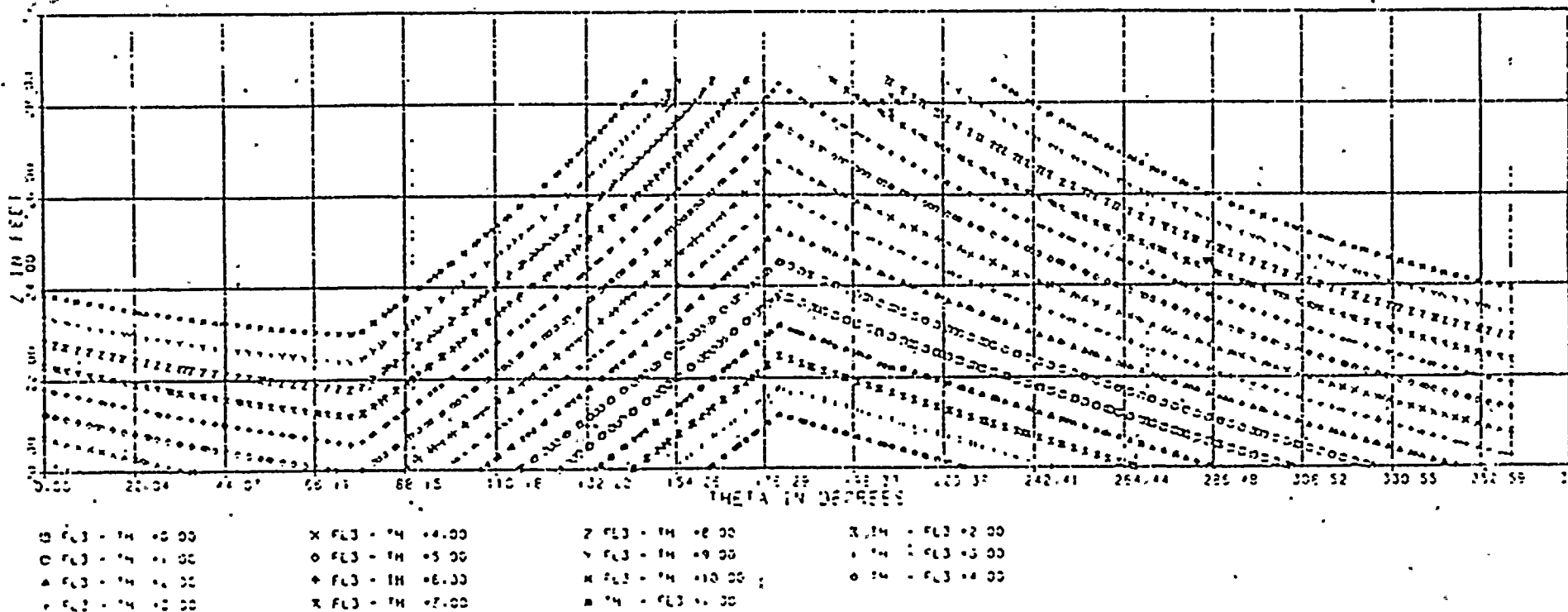


Figure A2. Family of FL3-TH Distance-Difference Curves



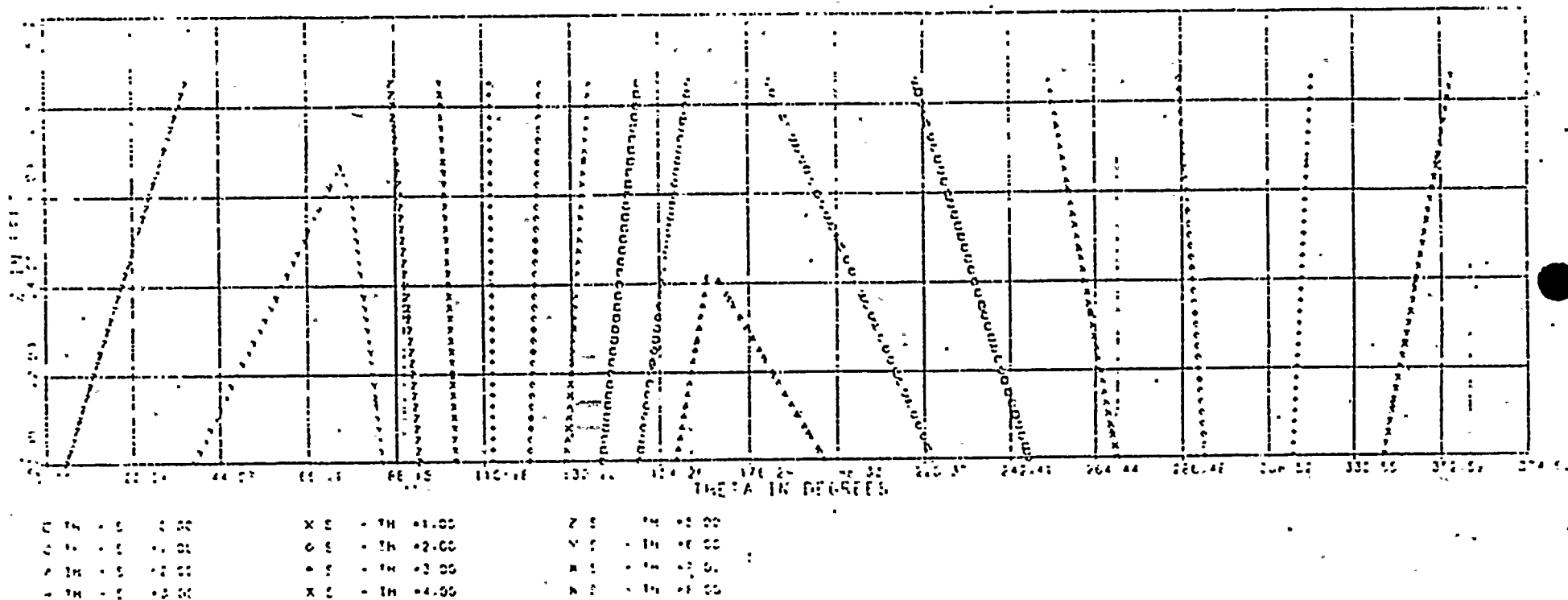


Figure A3. Family of S-TH Distance-Difference Curves



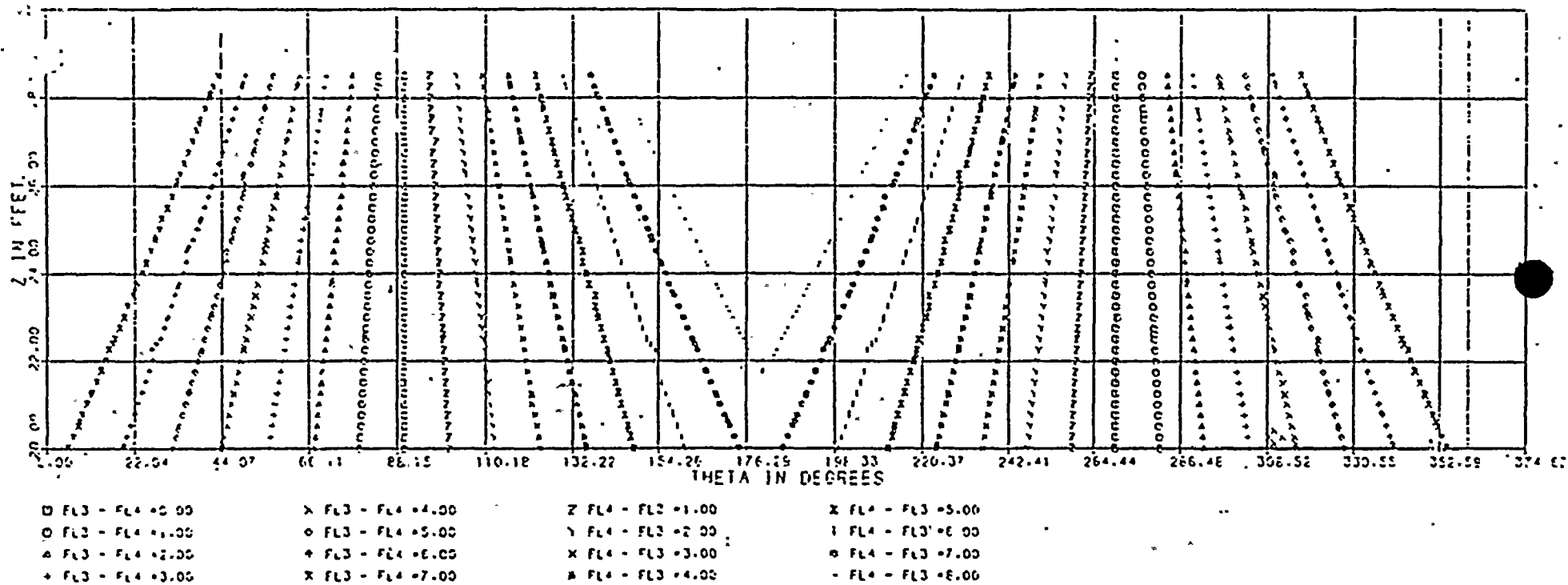


Figure A4. Family of FL3-FL4 Distance-Difference Curves

